

Supporting Information

Pump-to-Wheels Methane Emissions from the Heavy-Duty Transportation Sector

Nigel N. Clark†, David L. McKain†, Derek R. Johnson†, W. Scott Wayne†, Hailin Li†,
Vyacheslav Akkerman†, Cesar Sandoval†, April N. Covington†, Ronald A. Mongold†, John T.
Hailer†, Orlando J. Ugarte†*

†-Department of Mechanical and Aerospace Engineering, PO Box 6106, West Virginia
University, Morgantown, WV.

Corresponding Author: Nigel.Clark@mail.wvu.edu, 151B Engineering Sciences Building, 395
Evansdale Drive, Morgantown, WV 26505. Phone: 304-293-6457

Table of Contents

Pump-to-Wheels Methane Emissions Measurements	7
S1.1. Vehicle Emissions Measurement Methodology	7
S1.1.1. Measurement Uncertainty	7
S1.2. Quantifying Emissions at CNG and LNG Stations	10
S1.2.1. Full Flow Sampling System.....	10
S1.2.2. Leak Detection Methodology.....	11
S1.2.3. Leak Quantification Methodology	12
S1.3. LNG Stations	15
S1.3.1. LNG Station Model.....	15
S1.3.2. Thermodynamic Module.....	16
S1.3.3. Heat Transfer Model	17
S1.3.4. General Heat Transfer Approach	18
S1.3.5. Pressure Release Valve Module (Venting Model).....	19
S1.3.6. Model Scenarios.....	19
S1.3.7. LNG Deliveries	22
S1.3.8. LNG Station Boil-off Emissions	24
S1.3.9. LNG Station Leak Audit/Quantification Results	26
S1.3.10. LNG Vehicle Refueling	28
S1.3.11. LNG Station Leak Audit/Quantification Results Summary.....	28
S1.3.12. Manual Venting of LNG Tanks to Atmosphere.....	29
S1.3.13. Tank Venting Measurement and Analysis Methodology.....	30
S1.4. CNG Stations	35
S1.4.1. CNG Station Configurations	35
S1.4.2. CNG Station Leak Audit/Quantification Results	35
S1.4.3. CNG Vehicle Refueling	40
S1.4.4. Compressor Losses	41
S1.4.5. CNG Station Summary Results.....	44
S1.4.6. General CNG Station Observations	45
S1.5. Vehicle Performance and Engine Related Methane Emissions Data	46
S1.5.1. Data Processing.....	46
S1.5.2. Microtrip Averaged Results	46
S1.5.3. Vehicles with 9 Liter Stoichiometric NG Engines.....	47

S1.5.4. OTR Tractors with 9 Liter Stoichiometric NG Engines	48
S1.5.5. OTR Tractors with 12 Liter Stoichiometric NG Engines	50
S1.5.6. OTR Tractors with HPDI Engines	51
S1.5.7. Final Processed Vehicle Data	52
S1.6. Stasis Scenario to Estimate Emissions	57
S1.6.1 Vehicle Assumptions	57
S1.6.2 Station Population Assumptions	58
S1.6.3 Annual Vehicle Miles Traveled	59
S1.6.4 Station Assumptions	59
S1.6.5 Stasis Emissions Percentage by Component.....	60

Table of Figures

Figure S1-1: Full Flow Sampling System.....	10
Figure S1-2: FFS flow rate with 3/4 hp blower, 4” diameter intake hose ~35’ long.....	11
Figure S1-3: FFS used to measure methane emissions during an LNG tank refueling	13
Figure S1-4: Two-hour data collection associated with a time-fill compressor housing	14
Figure S1-5: Block Diagram of the LNG Fueling Station Model	16
Figure S1-6: Thermal resistance network for heat transfer through the LNG tank	18
Figure S1-7: Continuous pressure trace of an LNG station without a venting mitigation strategy	25
Figure S1-8: Continuous pressure trace of an LNG station with a venting mitigation strategy ...	26
Figure S1-9: LNG refueling summary	28
Figure S1-10: Distribution of manual venting dm/dP.....	32
Figure S1-11: Mass vented as a function of pressures and fill level.	33
Figure S1-12: WVU data set and additional data points.....	34
Figure S1-13: CNG refueling events at nozzle	41
Figure S1-14: CNG refueling events at vent.....	41
Figure S1-15: Natural gas compressor schematic (Picard, Ross, & Smith, 2002)	42
Figure S1-16: aero2 Pnumatic Actuators Performance Data during operation	44
Figure S1-17: Fuel energy vs average non-idle speed for all 9-liter stoichiometric engine powered vehicles. (n=2902).....	47
Figure S1-18: Fuel-specific tailpipe methane emissions vs average non-idle speed for all 9-liter stoichiometric NG engine powered vehicles. (n=1711)	47
Figure S1-19: Fuel-specific total (including tailpipe and crankcase) methane emissions vs average non-idle speed for all 9 Liter engine powered vehicles (n=1482).....	48
Figure S1-20: Fuel energy vs average non-idle speed for all 9-liter stoichiometric engine powered OTR tractors. (n=376).....	48
Figure S1-21: Fuel-specific tailpipe methane emissions vs average non-idle speed for all 9-liter stoichiometric NG engine powered OTR tractors. (n=167)	49
Figure S1-22: Fuel-specific total (including tailpipe and crankcase) methane emissions vs average non-idle speed for all 9 Liter engine powered OTR Tractors (n=225).....	49
Figure S1-23: Fuel energy vs average non-idle speed for all 12 liter stoichiometric engine powered OTR tractors (n=106).....	50
Figure S1-24: Fuel-specific tailpipe methane emissions vs average non-idle speed for all 12-liter stoichiometric NG engine powered OTR tractors. (n=93)	50
Figure S1-25: Fuel-specific total (including tailpipe and crankcase) methane emissions vs average non-idle speed for all 12 Liter stoichiometric NG engine powered OTR tractors (n=56)	51
Figure S1-26: Fuel energy vs average non-idle speed for all HPDI engine powered vehicles (n=142).....	51

Figure S1-27: Fuel-specific tailpipe methane emissions vs average non-idle speed for all HPDI engine powered vehicles (n=142)	52
---	----

Table of Tables

Table S1-1: Vehicle Characteristics for the HPDI and Stoichiometric Fleets.....	20
Table S1-2: Station Tank Parameters	20
Table S1-3: Station Tank Dimensions	20
Table S1-4: Station Piping Dimensions.....	21
Table S1-5: Solar loading and Ambient Temperature conditions	21
Table S1-6: Percentage of Utilization for HPDI and Stoichiometric Vehicles with Tanker Offload of 13,000 Gallons.....	22
Table S1-7: LNG Station Fuel Delivery Information	23
Table S1-8: LNG station summary.	28
Table S1-9: Estimated vent mass from on-board LNG tanks.	30
Table S1-10: CNG Station Audit Result Summary	45
Table S1-11: Bins of Average Speed for Each Activity	52
Table S1-12: Tailpipe and crankcase emissions and for three stoichiometric 9L transit buses ...	53
Table S1-13: Tailpipe and crankcase emissions and dsfc for five 9L stoichiometric refuse trucks	54
Table S1-14: Tailpipe and crankcase emissions and dsfc for three 9L stoichiometric OTR tractors	55
Table S1-15: Tailpipe and crankcase emissions and dsfc for three 12 L stoichiometric OTR tractors.....	55
Table S1-16: Tailpipe and crankcase emissions and dsfc for four 15 L HPDI OTR tractors.....	56
Table S1-17: Projected Population of NG Vehicles by Type	57
Table S1-18: Projected Population of NG OTR by Type	57
Table S1-19: Projected Population of NG Fuel Stations for HD Natural Gas Refuse Truck and Transit Bus	58
Table S1-20: Projected Population of NG Fuel Stations for HD OTR Trucks.....	58
Table S1-21: Projected Population of NG Fuel Stations for HD NG Vehicle Sector	59
Table S1-22: AVMT and Idle Time of Each Type of Vehicle	59
Table S1-23: Methane Emission for the Stasis Scenario	60

Pump-to-Wheels Methane Emissions Measurements

S1.1. *Vehicle Emissions Measurement Methodology*

Emissions and performance data were collected using a chassis dynamometer and/or through on-road testing with a portable emissions measurement system (PEMS).

The stoichiometric natural gas engines characterized, both 9 and 12 liter, had crankcases, which were vented to the atmosphere. This provided a pathway for methane in the engine intake fuel/air mixture that leaked into the crankcase past the piston rings to vent to the atmosphere and was a significant contributor to methane emissions from vehicles. Crankcase vent emissions from the first stoichiometric natural gas engines examined in the study were not characterized. However, for subsequent stoichiometric natural gas engine powered vehicle testing, crankcase emissions were either characterized using a separate full-scale dilution sampling system during chassis testing or by routing the crankcase vent to the exhaust such that an integrated engine-out+crankcase vent measurement was obtained. For on-road testing, additional test runs were performed to obtain tailpipe only methane emissions. Crankcase vent methane emissions were collected from two of the three dual-fuel retrofit engine powered vehicles during chassis testing. Crankcase methane emissions rates for HPDI engines were not significant compared to tailpipe methane emissions and were not characterized.

Fuel consumption for LNG and CNG fueled stoichiometric engine powered vehicles was determined using exhaust carbon balance methods where the fuel mass rate was calculated using the measured total carbon mass in the exhaust (in the form of carbon dioxide, carbon monoxide, and methane) arising from combustion and the carbon mass fraction for the particular fuel (0.747 grams C per gram of CNG, 0.749 grams C per gram of LNG).

Direct carbon balance fuel consumption determination was not possible for the dual-fuel retrofit and HPDI engine powered vehicles as carbon in the exhaust could arise from combustion of either diesel fuel or natural gas. For the dual-fuel retrofit vehicles, diesel fuel mass rates were determined using, either continuously recorded data from an external fuel supply or from continuously broadcast engine fueling data. The natural gas fuel rate was then determined through carbon balance methods using the carbon remaining (mainly CO₂) after the carbon arising from diesel fuel combustion was subtracted. A carbon mass fraction of 0.869 grams C per gram diesel fuel was used.

Diesel and LNG fuel consumption rates for HPDI engines were determined assuming that 10% of the fuel energy consumed was from diesel fuel at power and 42.5% of the fuel mass was from diesel at idle. These assumptions allowed for proportioning of the carbon in the exhaust and determination of separate diesel and LNG fuel consumption rates using carbon balance methods.

S1.1.1. Measurement Uncertainty

Methane and fuel consumption measurement uncertainties were, conservatively, set at +/-15% for measurements at idle and +/- 5% for measurements at power. An uncertainty analyses of data collected from a 9 liter stoichiometric engine powered OTR tested on a chassis dynamometer using a full-scale dilution sampling system indicated relative uncertainties for CO₂ measurements of

2.4% (UDDS) and 2.3% (HS Cruise), and uncertainty for CH₄ measurements of 2.8% (UDDS) and 2.4% (HS Cruise).

These values were obtained using a relative uncertainty of +/-1% for carbon dioxide concentration at or above 5,000 ppm, and absolute uncertainty of +/- 50 ppm for carbon dioxide concentrations below 5,000 ppm, a relative uncertainty of +/-1% for methane concentrations at or above 25 ppm, and an absolute uncertainty of +/-0.5 ppm for methane concentrations below 25 ppm. Additionally, the uncertainties for dilute exhaust measurement and dilution factor were assumed to be +/- 2%.

Uncertainty in the measured masses of methane or carbon dioxide was dependent on the uncertainty of the contribution made by ambient methane and carbon dioxide captured. While the absolute uncertainty of the background measurement was dominated by that from the total measurement at power, background measurement uncertainty had a significant influence at idle when lower total concentrations were observed.

The uncertainty for fuel measurements were not examined in detail. Fuel mass was reported based on exhaust carbon-balance (carbon dioxide was the dominant contributor by orders of magnitude over methane and carbon monoxide) and, variation in fuel carbon mass fraction would contribute but to a much lesser degree than carbon dioxide.

The contribution of relative uncertainty from background carbon dioxide and methane concentrations were significantly reduced for measurements using the PEMS system since it measures raw exhaust. However, uncertainty in measuring exhaust flow (+/- 5%) dominates emissions measurements.

Note that no run-to-run variability was included in measurement uncertainty. Issues such as coolant behavior, ambient temperature, catalyst behavior, and driver variability were not included in the uncertainties for fuel consumption and methane emissions.

The following citations provide additional insight into PEMS measurement uncertainty, but also incorporate uncertainty associated with use of brake-specific measurements:

- *Shimpi, S.A., "In-Use Emissions Testing – Engine Manufacturer's Perspective", Portable Emissions Measurement Systems Workshop, March 24, 2011*
(http://www.cert.ucr.edu/events/pems2011/05_Shirish%20Shimpi.pdf)
- *Rulemaking to consider Adoption of Gaseous Pollutant Measurement Allowance for California's Heavy-Duty Diesel In-Use Compliance Regulation, Public Hearing Notice and Related Material, Appendix C, Determination of Measurement Allowances through Laboratory Testing, Computer Modeling, and Over-the-road Testing Validation.*
(December 6, 2007). <http://www.arb.ca.gov/regact/2007/hdiuc07/appc.pdf>
- *Test Plan to Determine PEMS Measurement Allowance for the PM Emissions Regulated under the Manufacturer-Run Heavy-Duty Diesel Engine in-use Testing Program, Assessment and Standards Division, Office of Transportation and Air Quality, U.S. Environmental Protection Agency and California Air Resources Board and Engine Manufacturers Association, EPA-420-B-10-901, August 2010*
<http://www.epa.gov/otaq/regs/hd-hwy/inuse/420b10901.pdf>

- *Miller, J.W., Final Report Evaluation of Portable Emissions Measurement Systems (PEMS) for Inventory Purposes and the Not- To- Exceed Heavy- Duty Diesel Engine Regulation Contract No. 03- 345 June 2006.*
<http://cdm16254.contentdm.oclc.org/cdm/ref/collection/p178601ccp2/id/1542>

S1.2. Quantifying Emissions at CNG and LNG Stations

Introduction

Natural gas fueling stations were determined to be potential a source of methane emissions from the heavy-duty transportation sector. WVU characterized sources of methane emissions at eight, compressed natural gas (CNG) and six liquefied natural gas (LNG) fueling stations. These sources included leaks at fueling nozzles during vehicle refueling, losses at natural gas compressors, and leaks from fueling and fuel storage system components. Component leak detection and quantification was performed using a full flow sampling system (FFS) that was designed and developed by West Virginia University (WVU).

S1.2.1. Full Flow Sampling System

The FFS consisted of a hose that fed an explosive-proof blower that exhausted the collected sample through a mass airflow sensor (MAF) and sample probe. The sample probe was connected to a methane analyzer through a sampling tube. The system was instrumented with data logging equipment. The schematic of the FFS is shown below in Figure S1-1. Prior to operating the FFS, the grounding connection on the sampler hose was attached to a surface that allowed the system to be grounded. This was a preventive action to dissipate any static charge on the end of the hose, which could result from airflow through the hose.



Figure S1-1: Full Flow Sampling System

The sample intake hose was adjusted with respect to length and diameter in order to reach the leak location in question. The length and diameter of the sample intake hose had a direct influence on the flow rate of the system, as the pressure drop of the intake hose influenced total dilution flow. Regardless of the sample intake hose length, once configured the FFS produced a steady flow rate throughout the system. Figure S1-2 demonstrates the FFS flow when equipped with a $\frac{3}{4}$ horsepower (hp) blower and 4-inch diameter sample intake line, approximately 35 feet in length. Dependent upon the blower and hose configuration employed, the FFS was able to achieve a flow rate that ranged from 40-1500 SCFM.

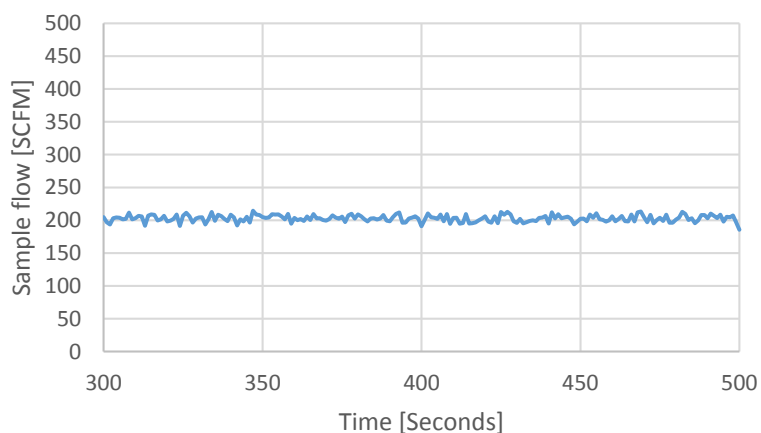


Figure S1-2: FFS flow rate with 3/4 hp blower, 4" diameter intake hose ~35' long

S1.2.2. Leak Detection Methodology

All interfaces that were safely accessible at a facility and presented the possibility of a natural gas leak were examined for the presence of a leak. Personnel that conducted the leak audit started by first surveying all potential leak sources before they proceeded with a leak detection survey. Inaccessible sources were documented.

Leak detection was concentration-based. WVU researchers used an Eagle II handheld methane detector from RKI Instruments. The handheld detector had a sensitivity of five parts per million (ppm). The handheld units were capable of measuring concentration up to 50,000 ppm. The instrument had a response time of approximately 15 seconds. The uncertainties of the units were +/-10%. Upon arrival to each site, a zero point calibration was performed on ambient air away from any possible leak sources. This allowed the device to detect any methane concentration above that of background. However, it was noted that this device was not used to quantify leaks and therefore did not affect the quantification of leaks.

The general procedure for detecting leak source locations was that the probe inlet of the handheld methane sensor was placed at the surface of the component interface where leakage would have likely occurred, and the probe moved slowly along the interface periphery, which ensured that the instrument's delayed response time was considered. For example, the detector tip was slowly passed along the length of a threaded joint between a pipe and fitting, and around the packing of a valve. If an increased meter reading occurred, the interface was slowly sampled until the maximum meter reading was obtained. The probe inlet was left at this maximum reading location for approximately two times the instrument response time. The maximum observed meter reading was noted and the leak location was marked for quantification using the FFS. In some instances, a soap-bubble solution was used in addition to the handheld methane analyzer, which aided in the identification of a leaking source in areas of densely populated pipefittings.

For this program, a leak was defined as any interface or source where methane concentrations observed using prescribed detection techniques exceeded 500 parts per million, which was

substantially above any background methane concentration drift. All source locations in which methane concentrations were observed were marked and the number of locations recorded. These source locations were quantified using the FFS, from largest to smallest, ensuring that at least 90% of the total site emissions were measured.

S1.2.3. Leak Quantification Methodology

The following was performed in cases where a source was classified as a leak based on detected methane concentration:

The location of the source, the methane concentration range detected, and any outside actions, which occurred at the time of measurement, were documented. Methane background concentrations were measured periodically throughout the site visit and with every leak quantification. The methane background concentration was subtracted from the sample flow concentration during post processing of the data. This was a preventative action to ensure that background concentrations did not influence the leak rate for specific leak source in question.

Each located leak source was quantified through the employment of the FFS. The sampling tube, or hose, was positioned at several points around the area of the leak source to obtain three consecutive leak rate quantifications for that source that included the continuously recorded sample flow and sample concentration. In some instances, the system was not stopped in between the three leak quantifications, and allowed to sample continuously. For continuous leak sources, the average observed concentration for the consecutive measurements were used to calculate the variance. If the variance in the measured leak concentration was greater than 10%, three additional quantifications were performed. If the variance was still above 10%, WVU personnel investigated to determine if the variance was the result of instrument malfunction or if the leak rate was variable. If the source of variability in leak rate was due to instrument malfunction, the source of malfunction was remedied and re-quantified, otherwise, the leak was classified as “variable”, and the suspected cause recorded.

In the case of multiple sources in close proximity or a single source enclosed by a covering, the source(s) in question were aggregated and treated as a single source for leak quantification using the enclosure. Depending upon the situation and leak location, the enclosure was fabricated entirely of plastic sheeting or incorporated either flexible, non-permeable material, or relying on a permanent enclosure such as a compressor housing. The enclosure allowed the quantification device to capture any natural gas that was leaking from components within its boundaries and allowed for dilution of the captured natural gas via purposely-placed holes in the enclosure or from existing vent locations on permanent enclosures. The duration of quantification sampling performed using an enclosure was dependent upon the size of the enclosure, allowing for any natural gas being diluted to be drawn from the enclosure and to achieve a steady reading from the LGR. The points at which the quantification sample was drawn from the enclosure and the dilution air was allowed to enter the enclosure, were situated such that the dilution air flowed across the potential leak source(s) to reduce the duration of sampling allowing for steady concentration

readings. The use of enclosures during this study was required at only CNG facilities. This was due, in part, to the fact that many compressors were housed such that direct access to individual leak sources, particularly packing vents, was restricted. In these specific instances, the compressor housing was sampled as a single unit by sealing off the compressor housing and using the FFS.

Figure S1-3 shows an example of an intermittent source of methane emissions. This example was for a refueling event. Background is shown from 150-240 seconds and from 425 seconds until the end. This particular event was for the refueling of a single LNG tank. The leak rate was integrated to determine the total mass emitted (9.5 grams).

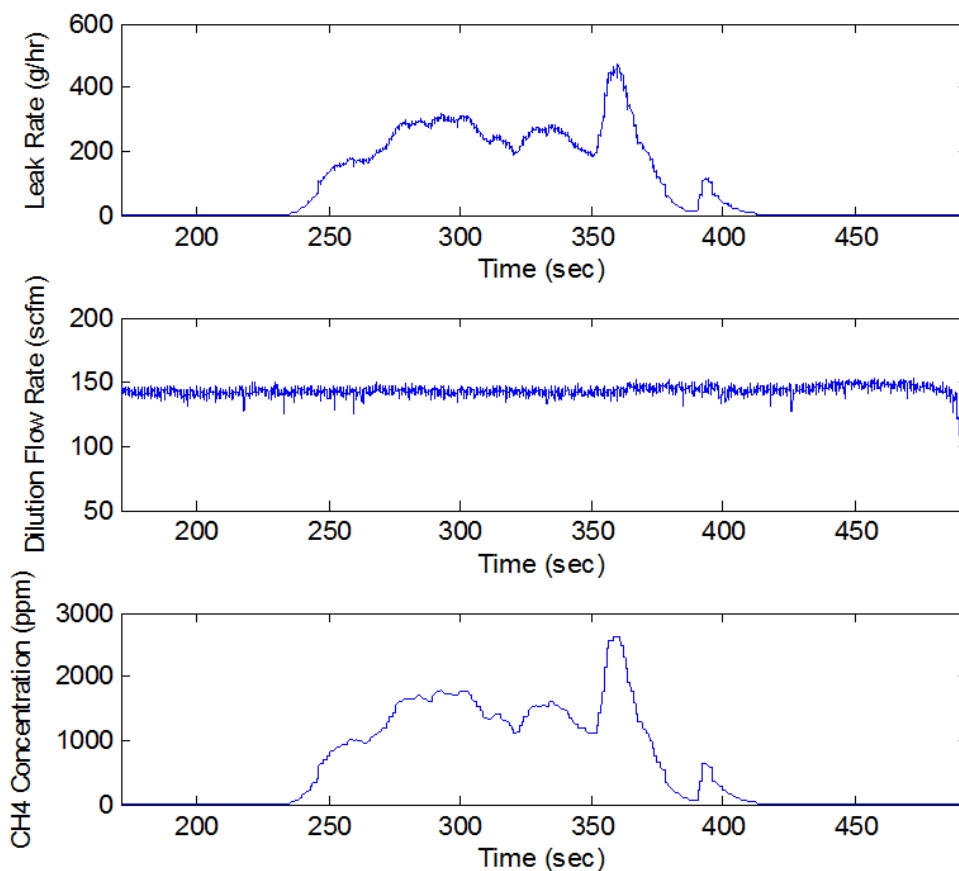


Figure S1-3: FFS used to measure methane emissions during an LNG tank refueling

Figure S1-4 shows an example of measuring the methane emissions from an aggregated source. These data were collected from a time-fill CNG compressor housing. Data were collected over two hours. Variations in leak rate and methane concentration were due to pressure fluctuations and variable leaks from compressor seals. For aggregated sources, data were collected for extended periods and the average leak rate was calculated.

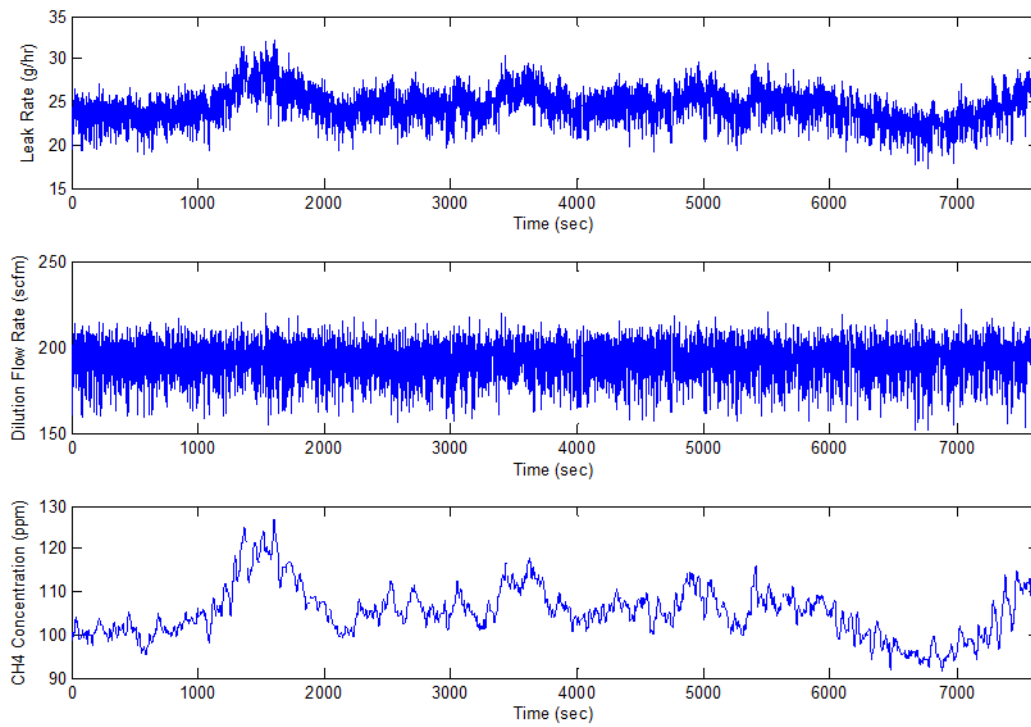


Figure S1-4: Two-hour data collection associated with a time-fill compressor housing

S1.3. LNG Stations

S1.3.1. LNG Station Model

A numerical LNG Fueling Station Model was developed in Simulink/MATLAB to estimate the mass of boil-off gas emitted to the atmosphere as a function of station design, operational parameters, and utilization. The model was divided into two main modules, the *Thermodynamic Module* and the *Heat Transfer Module*. The interactions of all the modules of the LNG fueling stations model are shown in Figure S1-5. The model was evaluated against long-term station pressure rise data collected. Tank pressure, fuel dispensing, and delivery data were gathered during three-week observation periods at two LNG stations for model validation. The model used the design configurations and the fueling use data from the two observed stations. Model results were compared to pressure rise rates measured over contiguous periods (37 to 91.5 hours) where activity did not include fuel deliveries to the station or venting. The model, on average, over predicted pressure rise by 19.7% with error from 0.7% under prediction to 37% over prediction. Model error was attributable to incomplete knowledge of station specifications, errors in estimating the mass/quality of vent gases returned to the station, and physical factors such as stratification in the tank. Losses due to transient cooling of lines were only approximately modeled. The model was subsequently used to predict the behavior of a reasonably representative station at different utilization levels, with the 19.7% correction applied.

The goal of the model was to evaluate pressure rise compared to threshold settings of pressure relief valves (PRVs). An additional model was developed which estimated the mass vented in the case that pressure reached this threshold and this mass was related to the total fuel consumed to present fuel specific emissions in the case of venting.

The *Thermodynamics Module* interacted with the *Heat Transfer Module* by providing the properties of the working fluid and conditions of the LNG tank. Heat transfer through the various plumbing and equipment in the LNG station was estimated by the *Heat Transfer Module*, which provided a heat input into *Thermodynamics Module*. During the next time step the *Thermodynamics Module* used the heat input to calculate the new pressure in the tank and give the *Heat Transfer Module* updated fluid properties and tank conditions. In this way, the Model marched through time to calculate pressure rise and boil of gas emissions (BOG).

In addition, there were other modules, which provided necessary information. For instance, the *Fleet* and the *LNG Dispenser* models interacted with each other providing information about the amount of mass exchanged between the station and vehicle because of dispensing fuel and vapor return from the vehicle tank to the station tank because of vapor balancing. These submodules provided information to the *Heat Transfer Model* module in order to calculate the heat transfer into the station tank when cooling down of the dispenser prior to dispensing fuel. Further, the *Fleet* model provided the temporal distribution of vehicle refueling activity experienced at the station.

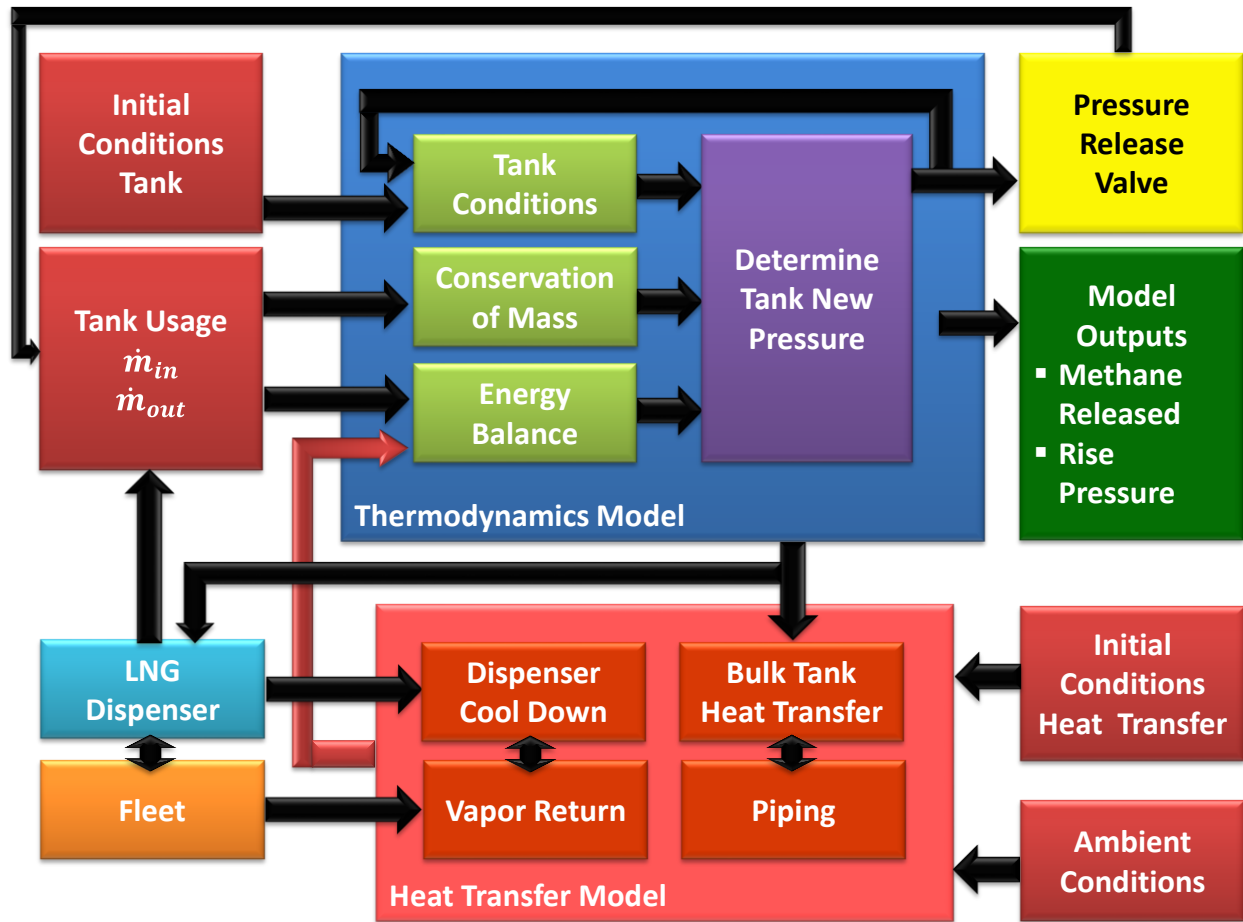


Figure S1-5: Block Diagram of the LNG Fueling Station Model

S1.3.2. Thermodynamic Module

The purpose of the thermodynamic model was to determine the thermodynamic state (pressure, temperature, specific volume) and properties (enthalpy, internal energy, specific heat, etc.) of the liquid and vapor phase methane in the storage tank in order to determine the rate of LNG boil off and venting. The detailed thermodynamic BOG model was developed, accounting for heat transfer through the tank shell and associated plumbing as a function of varying ambient conditions; varying mass flow of LNG into and out of the tank as a result of refueling the tank, fuel dispensing; recirculation to chill dispensing equipment; return of vapor from vehicle tanks for vapor balancing; and release of BOG to maintain safe tank operating pressure. The model employed differential forms of the energy balance, mass balance, thermodynamic property relations, and thermodynamic property data to describe the evolution of liquid and vapor quantity, state, and properties with time as a function of fueling station.

The following thermodynamic assumptions were used for the thermodynamics model of the LNG storage tank:

- LNG composition was 100% methane (CH₄). The effects of other constituents such as ethane, propane, butane, and carbon dioxide were not considered.
- Evaporation of LNG only occurred at the surface of the liquid phase.
- During the process of evaporation, the vapor-liquid phases were in thermodynamic quasi-equilibrium. Fast occurring transient behaviors transpiring during refilling or dispensing operations were not considered.
- The temperature and density of LNG was uniform throughout the liquid phase. Stratification of temperature, density, and other properties were not considered.
- Temperature and pressure in the tank were uniform.
- LNG could have been present in the tank as a liquid, vapor, or vapor-liquid mixture. If present as a mixture, the gas, and liquid were in phase equilibrium (both phases were saturated).
- Kinetic and potential energy of LNG flowing in and out of the tank were neglected.
- LNG was extracted or vented from the top of the tank as saturated gas and from the bottom of the tank as saturated liquid only.

In the interior of the thermodynamics model module there were four main concepts implemented. Three concepts were the equations that defined the tank conditions (including masses of vapor and liquid, vapor quality, and internal energy), the conservation of mass ($\frac{dm}{dt} = \sum \dot{m}_{in} - \sum \dot{m}_{out}$), and the energy balance ($\frac{dU}{dt} = \dot{Q} + \sum \dot{m}_{in} h_{in} - \sum \dot{m}_{out} h_{out}$). The fourth concept was the method to determine the new tank pressure, which fed the new tank pressure to the tank conditions block and updated every time step. Furthermore, the pressure of the tank was used in the pressure release valve block, which fed the tank usage block with the information necessary to keep the tank below the safe maximum pressure.

S1.3.3. Heat Transfer Model

The purpose of heat transfer module was to provide the total heat leak rate (\dot{Q}) to the energy balance block inside the thermodynamic model module. To do this calculation the heat transfer module modeled four main sources of heat leak into the cryogenic fluid. The sub-modules, which handled this, were the bulk tank heat transfer module, the piping module, the dispenser cool down module, and the vapor return module. The bulk tank heat transfer module used the current information of LNG liquid level and temperature from the thermodynamic model block, as well as the information provided from the initial conditions heat transfer block (including tank insulation thickness, cylindrical strut area ratio, and strut material conductivity) and the ambient conditions block (including ambient temperature, solar loading, and wind speed). The piping sub-module calculated the heat leak through the transfer lines between the bulk tank and the dispensers. The dispenser cool down module, modeled heat gained in the LNG transfer lines from cooling down a dispenser prior to use. When vehicles returned to a station to refuel, they occasionally were over pressurized and the station could not refuel them. LNG stations had a vapor return line from the vehicles. The vapor return module calculated the heat gain from the transfer line, normally a

bare pipe. Each of these modules was implemented using a general approach of 1-D algebraic heat transfer equations to approximate the heating load.

S1.3.4. General Heat Transfer Approach

Since the LNG was considered uniform and homogeneous, the objective of the heat transfer model was to provide the total heat leak rates into the LNG storage tank. The heat leak rates were then used in the thermodynamics model to determine the LNG boil-off rate, the corresponding pressure in the tank, the rate of release of BOG with the given PRV characteristics, and tank operating pressure limits.

To simplify the analysis a set of 1-D heat transfer equations were utilized. Resistance networks were created to allow the model to account for many different heat transfer modes. These networks were used in all the sub-modules. A thermal resistance network used for the bulk storage tank is shown in Figure S1-6.

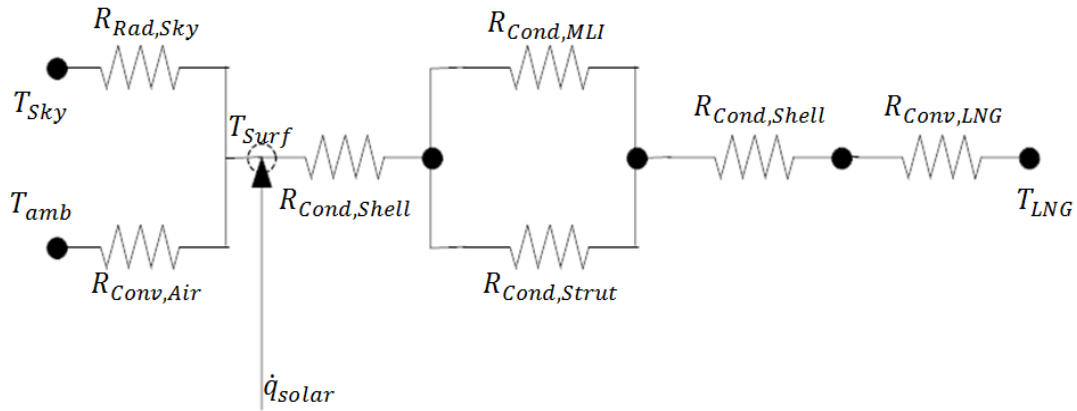


Figure S1-6: Thermal resistance network for heat transfer through the LNG tank

Similar resistance networks were developed for the other sub-modules and their respective parts. Thermal conductivity was taken to be a function of temperature and was updated in the equations every time step.

Below is a list of important assumptions and simplifications used in the heat transfer module.

- Valves and fixtures in the LNG transfer lines were modeled by using equivalent length piping in the piping sub-module.
- Dispensers were modeled using their internal piping only ignoring any supporting structures inside in the dispenser cool down sub-module.

The vapor return sub-module used an incompressible flow approach to calculate the mass flow rate through the vapor return line during a vehicle-fueling event.

S1.3.5. Pressure Release Valve Module (Venting Model)

The LNG tank-venting model calculated the mass of vapor that needed to be removed from a LNG tank in order to drop the pressure from an initial pressure (P_{pre}) to a desired final pressure (P_{after}). This component of the LNG station model was used to estimate the mass of vapor that was transferred from a vehicle tank to the station tank during vapor balancing. It was also used to estimate the mass of vapor released from the PRV in the event that the PRV activation pressure was reached.

The model assumed isothermal homogenous conditions within the tank during this venting stage. Additionally, potential and kinetic energy, work, and heat transfer were neglected.

The volume of the tank (V_{tank}), total initial mass of methane in the tank ($m_{total,pre}$), the initial pressure (P_{pre}), and the final pressure (P_{after}) were required as input to the calculations. These values were computed by separate components of the overall model. The mass flow rate of BOG released through the vent valves ($\dot{m}_{out,g,vent}$) was defined as the total mass released ($m_{out,g} = m_{total,pre} - m_{total,after}$) in a time step size, Equation S1-1:

$$\dot{m}_{out,g,vent} = \frac{m_{out,g}}{\Delta t} \quad \text{Equation S1-1}$$

S1.3.6. Model Scenarios

Based on data available from audited LNG stations, a representative station was defined to estimate current or future LNG station emissions. However, LNG station were complex dynamically dependent systems, station design (dimensions), management processes, and/or fleet behavior drastically affect its emissions and pressure rise rate. The following representative station and utilization demographics were used in the model to evaluate the effect of station utilization on BOG emission rate.

The following sections represent the baseline scenario for HPDI and Stoichiometric vehicle fleets at the specific representative station.

Vehicles

Table S1-1 describes the characteristics for the HPDI and Stoichiometric vehicles used in the scenarios.

Table S1-1: Vehicle Characteristics for the HPDI and Stoichiometric Fleets

Type of Vehicles Fleet	HPDI	Stoichiometric
Vehicles Tanks	1: 190 gal	1: 190 gal
Arrival Pressure	170 psig	130 psig
Arrival Level	30%	30%
Pressure after Venting	120 psig	NA
Final Level after Dispensing	90%	90%
Fuel Dispensed	114 gal	114 gal

Station Tank

One vertical station LNG tank of 25,000 gallons was used for all the scenarios simulations, however, initial and final pressure were different when HPDI or Stoichiometric vehicles were used. Table S1-2 and Table S1-3 summarize the tank characteristics and dimensions, as well as the initial and final pressure allowed per vehicle type.

Table S1-2: Station Tank Parameters

Number of Tanks	1	
Orientation	Vertical	
Capacity	25000 gallons	
Fleet	HPDI	Stoichiometric
Initial Pressure	65 psig	80 psig
Max. Pressure	135 psig	150 psig
PRV Drop Pressure	1 psig	
Initial Level	90%	

Table S1-3: Station Tank Dimensions

Model Station Bulk Tank Dimensions		
Orientation	vertical	
Dimension	value	unit
Volume	94.635	m ³
Outside Diameter	3.000	m
Inner Diameter	2.540	m
Height	20.320	m
Inner Wall Thickness	0.025	m
Outer Wall Thickness	0.025	m

Station Piping

The station piping for each section of the piping was modeled as an equivalent length of piping distributed (by percentage) among the following piping types - in order to allow the station to be easily scaled. The station piping dimensions are shown in Table S1-4

Table S1-4: Station Piping Dimensions

Model Station Pipe Composition					
Recirculation/Dispenser Supply Piping (equivalent length = 75 meters)					
Nominal Diameter (in)	Schedule	Material	Insulation	Percent Composition	Length (m)
2.5	10	s.s.	VJP	65.00%	48.75
2	10	s.s.	VJP	15.00%	11.25
2	10	s.s.	Rigid Foam	10.00%	6.75
1.5	10	s.s.	Rigid Foam	9.00%	6.75
1	10	s.s.	none	1.00%	0.75
Dispenser # 1 Piping (equivalent length = 4 meters)					
1.5	10	s.s.	VJP	25.00%	1
1	10	s.s.	none	75.00%	3
Vapor Return Piping (equivalent length = 20 meters)					
1	10	s.s.	none	100.00%	20

Weather Conditions

The model accounted for varying ambient conditions. Table S1-5 illustrates the assumed representative conditions. Ambient temperature was input as a sinusoidal wave with the peak temperature at 1 pm and the low at 1 am. Solar loading raised from zero to the peak solar loading values along an inverted parabolic path then back to zero during a twelve-hour window.

Table S1-5: Solar loading and Ambient Temperature conditions

Ambient Temperature	286 K \pm 10 K
Peak Direct Solar Loading	900 W/m ²
Peak Diffuse Solar Loading	90 W/m ²

Fleet behavior

Total number of vehicles arriving at the station for refueling was assumed to be evenly spaced during each day. The numbers of vehicles used were from two up to 130 per day.

Utilization

Equation S1-2 defines the percentage of utilization:

$$\%Utilization = \frac{\#Vehicles * Fuel Delivered per Vehicle (gal)}{Tanker Offload (gal)} \quad \text{Equation S1-2}$$

A typical LNG tanker that offloads to a station carries 10,000 or 13,000 gallons of LNG. Normally tankers did not deliver partial loads. The definition of 100% utilization was then the maximum number of vehicles that were filled from this quantity of LNG in a day. In this way, 100% utilization always has the same meaning when referring to a specific amount of LNG. A 25,000 gallons station tank has a capacity of 22,500 gallons (because of ullage volume) of LNG and

received an offload of 13,000 gallons of LNG taking the bulk tank from ~38% to ~90% fill level. The following table shows the percentage of utilization for HPDI and Stoichiometric vehicles with a tanker offload of 13,000 gallons.

Table S1-6: Percentage of Utilization for HPDI and Stoichiometric Vehicles with Tanker Offload of 13,000 Gallons

# Vehicles		Fuel Dispensed per Day (gal)		Percent Utilization (%)	
HPDI	Stoichiometric	HPDI	Stoichiometric	HPDI	Stoichiometric
2	2	228	228	1.75%	1.75%
4	4	456	456	3.51%	3.51%
6	6	684	684	5.26%	5.26%
8	8	912	912	7.02%	7.02%
10	10	1140	1140	8.77%	8.77%
11	11	1254	1254	9.65%	9.65%
12	12	1368	1368	10.52%	10.52%
13	13	1482	1482	11.40%	11.40%
14	14	1596	1596	12.28%	12.28%
15	15	1710	1710	13.15%	13.15%
20	20	2280	2280	17.54%	17.54%
25	25	2850	2850	21.92%	21.92%
30	30	3420	3420	26.31%	26.31%
35	35	3990	3990	30.69%	30.69%
40	40	4560	4560	35.08%	35.08%

These percentages of utilization were used as inputs into the model to calculate the percentage of fuel lost due to BOG venting. The percentage of fuel lost to BOG is defined by Equation S1-3:

$$\begin{aligned} \text{\%Fuel Lost to BOG} \\ = \frac{\text{Fuel Vented (kg)}}{\text{Tanker Offload (kg)}} \end{aligned} \quad \text{Equation S1-3}$$

Where the tanker offload was converted from gallons into kilograms using the density of the liquid methane at the initial pressure of the respective bulk tank simulation.

S1.3.7. LNG Deliveries

West Virginia University (WVU) personnel witnessed six bulk fuel delivery offloads to a facility that employed the most recent refueling technology. This recent refueling design did not require the venting of the refueling lines after completion of the offload. When everything worked properly and the delivery driver followed all of the directions exactly as requested by site personnel this new design yielded a minimal amount of methane (~ 1 cubic feet of liquid) to be released. This equates to around 11.1 kg of methane assuming that the liquid was saturated at the average post pressure (44 PSIG). The amount released increased when the operator did not follow the stated directions. However, the increased amount was not comparable to that released during a

bulk fuel offload employing the “old” system in which the lines were required to be drained. Table S1-7 displays the tank pressure of the fuel delivery truck before and after the bulk fuel delivery.

Table S1-7: LNG Station Fuel Delivery Information

Delivery		Truck	
		[PSIG]	[inH2O]
1	Pre	6	25
	Post	42	5
2	Pre	15	27
	Post	44	4
3	Pre	9	16383 gal
	Post	49	8.5
4	Pre	-	-
	Post	40	3
5	Pre	14	26
	Post	45	0
	Post vent	21	0
6	Pre	29	27
	Post	55	6

It should be noted that the fifth LNG delivery driver did not follow standard operating procedures. This yielded an additional methane loss due to venting. The driver vented down the entire filter system to save time due to accumulation of an air pocket in the system during recirculation and an 8ft section of 0.5 inch diameter hose equating to ~25 cubic feet of methane vapor being released to the atmosphere. Assuming only vapor was released at the saturation pressure of 45 PSIG; this would have yielded an additional methane loss of 4.7 kg. After the offload was complete, the truck vented off 24 PSI (from 45 PSIG to 21 PSIG) through the stack in addition to the typical amount of liquid loss (11.1 kg from calculation above). The tank was noted to have a maximum load capacity of 35,000 pounds and this equates to a tank volume of 10,439 gallons from saturated LNG at 14 PSIG. However, the actual volume of the inner tank would be required for a final calculation and it was noted that 10,439 gallons was lower than the volume presented to WVU researchers' onsite. It was noted that the site level gauge indicated zero liquid level and therefore the amount of methane in the tank was calculated based on the entire tanker containing only saturated vapor at an initial pressure of 45 PSIG and final pressure of 21 PSIG. This equates to a mass vented of 45.7 kg. Therefore, it was estimated that 61.5 kg of methane was lost during this bulk fuel offload event. The total fuel transferred during this delivery was 16,181 kg and this loss represents 0.38% of the delivered value. If the additional five fuel transfers only lost the estimated value of 11.1 kg, the total methane loss for these five deliveries was 117.0 kg. The total amount of LNG transferred for these six deliveries was 87,945 kg. Therefore, these losses represent 0.128% of the delivered fuel (1.3 g/kg). Additional minor losses and venting did occur but estimates were not given for these occurrences. Any additional losses that occur after the tankers left the station perimeter was not known.

LNG Delivery Loss Estimates

Based on WVU observations the LNG loss during bulk delivery should typically be 11.1 kg based on the loss of about 1 cubic foot of LNG (liquid phase). The average LNG delivered for these six

station refueling was 14,658 kg. Therefore, under normal conditions this would represent a loss of 0.08% or 0.8 g/kg. One of the six (16.7%) refueling events observed had higher than typical losses. The initial estimate for these losses was 61.5 kg for a transfer of 16,181 kg equating to a loss of 0.38% or 3.8 g/kg. For this event, this value was above the initial WVU threshold of significance of 2.5 g/kg. It was concluded that these additional higher than normal losses would need to occur 56.7% of the time for the overall loss per station delivery to be significant (2.5 g/kg).

Summary of Events:

Refuel 1: 11.1 kg loss, 14361 kg, 0.77 g/kg

Refuel 2: 11.1 kg loss, 14569 kg, 0.76 g/kg

Refuel 3: 11.1 kg loss, 12828 kg, 0.86 g/kg

Refuel 4: 11.1 kg loss, 15622 kg, 0.71 g/kg

Refuel 5: 61.5 kg loss, 16148 kg, 3.81 g/kg

Refuel 6: 11.1 kg loss, 14234 kg, 0.78 g/kg

Uncertainty in LNG deliveries

Losses were based on volumes of hardware that was vented and pressures that were noted from the delivery tankers mechanical pressure gauge. In all cases, this involved the connector volume. The uncertainty in volume due to variations in production geometry or shrinkage due to temperature was not known. The uncertainty in volume was also based on estimated measurements as site personnel were not allowed to measure or photograph components, or quantify methane losses during bulk fuel deliveries. As such, these uncertainties were unknown. An additional uncertainty was due to the notation of the pressure measurement gauge. The uncertainty arises in the assumption of vented vapor or liquid as being saturated at the pressure indicated by the tanker pressure gauge. This pressure was measured by visual inspection and WVU feels that a sight uncertainty of +/-1 PSI existed. In the standard case of a loss of one cubic feet of liquid, the mass loss would be approximately 11.1 +/- 0.03 kg. In the single case where venting occurred the total mass lost was 61.5 +/-0.2 kg.

S1.3.8. LNG Station Boil-off Emissions

Observed LNG Station Boil-off Emissions

LNG storage tank pressure was monitored continuously during two three-week observation periods, at two different LNG stations. Observed pressure and utilization data were used to verify and improve the theoretical pressure rise model developed during the research effort. However, certain pressure and utilization data were not appropriate for model validation as these data were influenced by events that the model did not incorporate. These data included observations during and immediately after bulk fueling of the station since the exact condition (temperature, pressure) was not known. Data excluded from use in model validation also included periods where regulated or manual venting of the bulk tanks occurred since the mass rate of fuel leaving the tank was not known. Figure S1-7 shows storage tank pressure over the three-week observation period at one of

the LNG station. Tank pressure at this station was managed by venting gaseous methane to the atmosphere through a regulator when tank pressure reached a particular set point (~135 PSIG). The average throughput of this station was 1,538 DGE/day. The constant downward slope centered on day 11 shows a venting period where methane was being vented to the atmosphere and lasted 26.5 hours. Figure S1-7 also shows that station pressure was at or near venting pressure during the night of day 15 but a delivery of LNG decreased station pressure and vent any vent duration was not known.

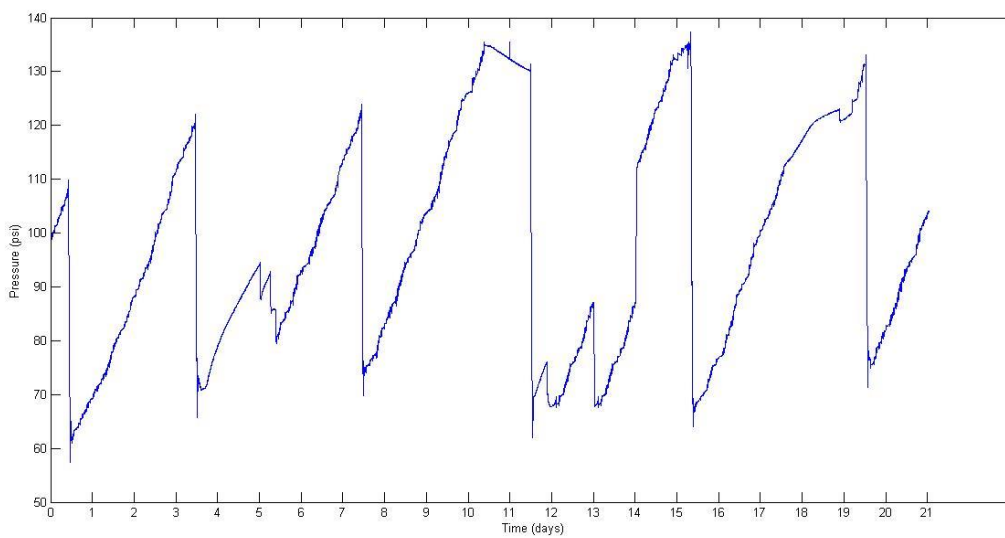


Figure S1-7: Continuous pressure trace of an LNG station without a venting mitigation strategy

Figure S1-8 illustrates storage tanks pressure over the three-week observation period for the second LNG station. Tank pressure at this station was typically managed by venting methane to a natural gas powered generator, which in turn, feed into the local electrical grid. However, during the observation period, the generator was down for maintenance (day 4-10) and station tank pressure had to be managed by manually venting methane gas to the atmosphere. These manual venting events correspond to the rapid pressure drops in Figure S1-7 on day 3, 4, and 17. The pressure drops in Figure S1-8 occurring on day 8, 12, and 18 corresponds to a bulk fuel delivery. The average throughput of this station was 701 DGE/day.

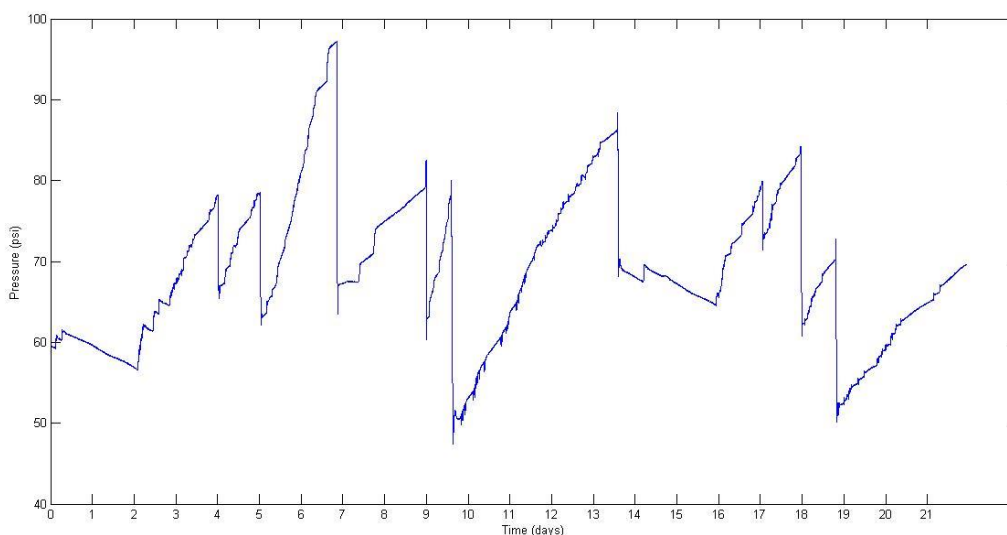


Figure S1-8: Continuous pressure trace of an LNG station with a venting mitigation strategy

LNG Stations Continuous and Nozzle Emissions

All LNG fueling facilities that participated in the study utilized liquid natural gas delivered by truck from a liquefaction processing plant.

S1.3.9. LNG Station Leak Audit/Quantification Results

LNG Station No.1

LNG Station No.1 was a public facility that provided LNG to a commercial vehicle fleet, seven days a week and was equipped to supply CNG. The facility was equipped with two dispensers employing an older generation nozzle design. The facility indicated that nozzles of this design were in the process of being phased out of the industry.

The fueling station had a vertical storage tank. WVU researchers were unable to fully capture any refueling events due to the amount of leakage occurring at the nozzle. The amount of leakage occurring at the two partially captured refueling events was at a minimum of 2 kg/hr. During the station audit, one leak was located and quantified at the packing of an actuated valve (53.06 g/hr), this was corrected with the tightening of the packing by a quarter turn.

LNG Station No.2

LNG Station No.2 was a public facility that provided LNG to a commercial vehicle fleet, seven days a week. The facility was equipped with two dispensers.

The fueling station had a horizontal storage tank. Refueling events were captured from 19 vehicles. During the station audit, three leak sources were located and quantified. After being measured, the leaks were corrected by tightening the fittings. The continuous leaks measured had a leak rate of 0.92 g/hr. Of the leak sources quantified, the minimum, maximum, and average values were 0.1, 0.5, and 0.3 g/hr.

LNG Station No.3

LNG Station No.3 was a public facility that provided LNG to a commercial vehicle fleet, seven days a week. The facility was equipped with two dispensers.

The fueling station had a vertical storage tank. This facility employed a venting management strategy. During the station audit, three leak sources were located and quantified. The continuous leaks measured had a leak rate of 0.24 g/hr. Of the leak sources quantified, the minimum, maximum, and average values were 0.02, 0.22, and 0.08. WVU researchers conducted four measurements of refueling events. However, upon further analysis of the data these measurements were excluded from analysis due a suspected analyzer error.

LNG Station No.4

LNG Station No.4 was a public facility that provided LNG to a commercial vehicle fleet, seven days a week. The facility was equipped with two dispensers.

This facility contained two vertical tanks. This station was originally designed to provide both warm and cold (saturated and unsaturated fuel) fuel to vehicles. Due to the current customer base, however, this facility currently only provides cold fuel. This change has led this facility to enact a venting management strategy utilizing existing equipment on site. During the station audit, two leak sources were located and quantified. The continuous leaks measured had a leak rate of 16.62 g/hr. The located leaks were the result of station maintenance occurring the day of the audit in which two compression fittings were not fully tightened. After the located leaks were measured, the fittings were tightened and then re-measured. The tightening of the fittings stopped any leakage from occurring. Of the leak sources quantified, the minimum, maximum, and average values were 8.30, 8.33, and 8.31 g/hr. Refueling events were captured from seven vehicles.

LNG Station No.5

LNG Station No.5 was a public facility that provided LNG to a commercial vehicle fleet, six days a week. The facility was equipped with two dispensers. This facility had personnel onsite at all times.

This facility contained one vertical 15,000-gallon tank and employed a venting management strategy. During the station audit, six leak sources were located and three were quantified. The continuous leaks measured had a leak rate of 5.97 g/hr. Of the leak sources quantified, the minimum, maximum, and average values were 0.69, 3.12, and 1.99 g/hr. Refueling events were captured from seven vehicles.

LNG Station No.6

LNG Station No.6 was a private facility that provided LNG to a commercial vehicle fleet, six days a week. The facility was a terminal station equipped with one dispenser. This facility had personnel onsite at all times.

This facility contained one horizontal 15,000-gallon tank. During the station audit, one leak source was located and quantified. The continuous leak measured had a leak rate of 0.01 g/hr. Refueling events were captured from nine vehicles.

S1.3.10. LNG Vehicle Refueling

LNG refueling events were captured from 43 HPDI heavy-duty vehicles. Not all of the refueling events collected from dispensers employing the older generation nozzle design were included as the measured value exceeded the measurement range of the analyzer. The facilities employing that nozzle design indicated that that technology was currently in the process of being phased out and thus not representative of the current industry norm.

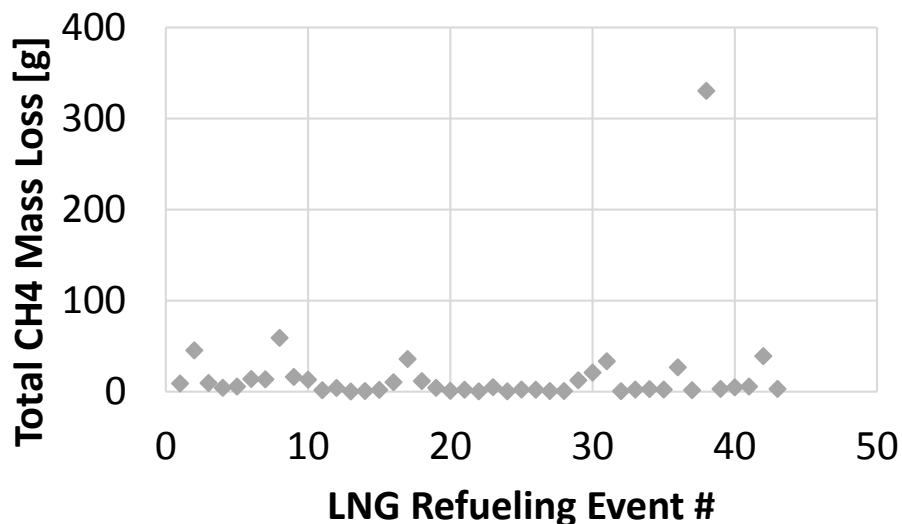


Figure S1-9: LNG refueling summary

The LNG refueling event measured at 330.4 g/event was a minimal estimate of a refueling event. WVU researchers were unable to capture the entire refueling event due to the amount of liquid emanating from the nozzle. The minimum, maximum, and average values occurring at the nozzle were respectively, 0.12, 330.4, and 17.7 g/event. Excluding the estimate, the minimum, maximum, and average values occurring at the nozzle were respectively, 0.12, 59.06, and 10.26 g/event.

S1.3.11. LNG Station Leak Audit/Quantification Results Summary

The summary of LNG short-term station audits completed is shown in Table S1-8.

Table S1-8: LNG station summary.

Station Type			Continuous Leaks [g/hr]
1	OTR	Public	53.1
2	OTR	Public	0.9
3	OTR	Public	0.2
4	OTR	Public	16.6
5	OTR	Public	6.0
6	OTR	Public	0.0

LNG refueling events were captured from 43 HPDI heavy-duty vehicles with an average leak rate of 17.7g per refueling event.

Every leak located at a LNG facility in this study was classified as occurring from an unintentional leak source.

For this study, the following conversions were used for natural gas for transformation from a volume to a mass basis:

1 GGE = 5.66 lb natural gas (NIST Handbook 44)

1 DGE = 6.06 lb natural gas (GNA, NGVC, CVEF, Encana, CHK consensus)

S1.3.12. Manual Venting of LNG Tanks to Atmosphere

WVU investigated the level of significance for LNG tank venting. Specifically, the percentage of the fleet venting a specific amount of fuel per event to the atmosphere was at levels comparable to other sources of methane emissions from the heavy-duty transportation sector. This task was accomplished through the estimation of the mass released during venting based on experimental results and the application of the estimates to real-world observations.

Estimating Vent Mass

It was difficult to quantify directly, the mass of methane released to the atmosphere when an in-use LNG tank was vented due to the large mass rates encountered. While this was initially not an objective of the program, WVU did collect vent rate data from both Chart and Westport vehicular LNG tanks during pressure-rise experiments while venting the tanks to reduce fuel levels. During these experiments, the mass of the tank was continuously monitored such that direct vent mass rates were recorded. In addition to these data, Clean Energy collected and shared data from their own in-house observations of LNG tank venting and data from a Westport LNG tank were available in the public domain.

Observed On-Board LNG Tank Venting

WVU observed and was able to obtain complete data from venting for six vehicles at a single LNG station that included venting from ten individual vehicular LNG tanks. The estimated mass vented for each tank-venting event was calculated as a function of initial and final tank pressure and initial fill level using the empirical equation developed using experimental vent data and was included in the table.

Initially the methane vented from these tanks was based on an average methane vent rate of 0.1664 kg/PSI, which was based on averages from the original WVU experimental data set. The vent masses have been recalculated using the empirical model of Figure 3 developed using WVU, NorthStar, and Westport data.

Tank Level Estimation

In order to utilize this model the initial mass of fuel in the tank (as a percentage of mass for a full tank excluding ullage) was necessary. For the six vehicles (ten tanks), the fill levels were read from the fuel gauges in each vehicle. However, these values were not consistent with fueling records for the vehicles. For example, one of the vehicle tanks indicated 12.5% fuel level (the gauge was readable to eight segments/nine levels) which, based on a full tank mass of ~183 kg, would represent 22.9 kg. Fueling data for this vehicle showed that ~44 DGE (121 kg) of fuel were

required to “fill” the vehicle, which would imply that the tank level on arrival was 34%. The mass of methane vented from these six vehicles (ten tanks) were estimated using both the indicated and inferred tank levels. It has been established that the tank level gauges were not always accurate.

Additionally, the fueling records did not contain data for individual tanks as the typical fill operation involved a single transaction but included filling two tanks. However, vehicle fuel consumption management appeared to maintain similar levels for the two tanks and most two-tank vehicles were observed to have the same percent fuel level in each of their tanks. As such, the inferred tank levels were based on apportioning the delivered fuel based on the difference in tank volumes (62% for driver side tank (119 gallon), 38% for passenger (70 gallon)).

Results

The vent masses estimated using the revised empirical model was lower than those from the original differential pressure model were. The average estimated mass lost during venting for the six vehicles that were observed and characterized was 5.0 kg per tank, which equated to 48.8 g/kg of fuel delivered. Five of the six vehicles had two tanks but WVU was not able to characterize the passenger tanks on one of the six vehicles.

Table S1-9: Estimated vent mass from on-board LNG tanks.

Vehicle #	Tank	Pressure Before Vent (PSIG)	Pressure After Vent (PSIG)	% Fill from Gauge	% Fill from Fueling	Old Average Method (kg)	New Mass Vented from Gauge (kg)	New Mass Vented from Gauge (g/kg)	New Mass Vented from Fueling (kg)	New Mass Vented from Fueling (g/kg)
265	1	228	105	13%	34%	20.9	3.1	25.9	9.5	78.6
265	2	235	123	13%	34%	18.6	2.8	38.9	8.4	118.4
313	1	170	59	13%	27%	18.5	3.3	24.4	7.7	58.0
313	2	170	60	13%	27%	18.3	3.2	41.1	7.6	97.6
318	1	167	152	25%	13%	2.5	0.8	4.8	0.4	2.3
314	1	185	45	6%	12%	23.3	1.8	11.1	3.9	24.4
314	2	190	55	25%	12%	22.5	8.4	88.7	3.7	39.3
336	1	220	150	6%	26%	11.6	0.7	5.5	3.8	28.0
336	2	202	150	25%	13%	8.7	2.8	29.6	1.3	13.9
379	1	230	175	33%	31%	9.2	3.8	29.9	3.5	27.9
Average		200	107	17%	23%	15.4	3.1	30.0	5.0	48.8

S1.3.13. Tank Venting Measurement and Analysis Methodology

For pressure-rise model verification experiments, tank pressure was allowed to rise to the pressure relief valve setting. After necessary data were collected, (some PRV activity data were obtained and analyzed) the tanks were manually vented to the atmosphere to reduce the fuel level in the tank in preparation for subsequent pressure-rise work. These manual venting operations were performed in single or multiple steps while tank weight was continuously recorded. For the

pressure-rise verification work, WVU gathered data from near-full tanks and, as a result, did collect some vent mass data while reducing tank level from near-full conditions. This point would not be representative of real world venting since vehicular tanks would normally be vented prior to fueling where near-full conditions would not be expected.

Results

Eight manual ventings of a Chart tank and five manual ventings of a Westport HPDI tank were characterized. Each of these ventings included a full characterization from pressures near the PRV set point down, eventually, to atmospheric pressure. Most of these characterizations included multiple venting segments. For example, one complete venting of the Chart tank included four individual segments where the tank pressure was incrementally dropped from 263 psia to 20 psia and the tank was allowed to “rest” after each segment. These segments may be more representative of real-world venting scenarios. Plots are also presented that show the linear regressions as applied to each event. Data were collected on 31 vent segments. The minimum, maximum, and average of these mass loss per pressure vented (kg/psi) were 0.07, 0.39, and 0.18, respectively.

Since there were more than 10 data points, an outlier analysis was performed using the criteria of \pm two standard deviations of the average. The standard deviation of the complete data set was found to be 0.08. The two maximum ratios were determined to be possible outliers and were removed from the analysis. The minimum, maximum, and average values for the remaining 29 data points were 0.07, 0.29, and 0.17 kg/psi, respectively. The distribution of the remaining 29 data points is shown in Figure S1-9. It was noted that the median of this data set was 0.17 kg/psi. The R-squared values were between 0.9205 and 0.9991 for this linear regression analysis. Therefore, on average a tank would vent 0.17 kg of methane for every PSI of vented tank pressure.

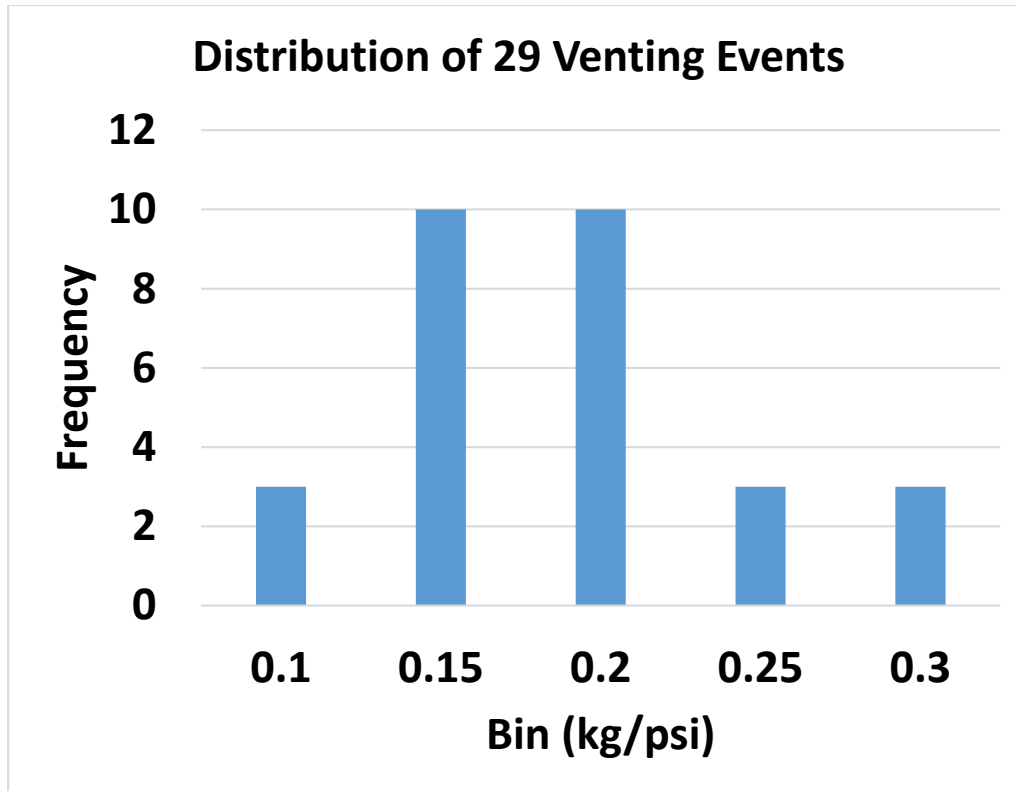


Figure S1-10: Distribution of manual venting dm/dP .

Empirical Analyses

Figure S1-11 shows the amount of mass vented in kilograms plotted against a ratio of the vented differential pressure to the square root of initial tank pressure multiplied by a mass percentage of fill.

$$\left(\frac{dP}{\sqrt{P_i}} \right) \times \% \text{ Fill}$$

Where

$$\% \text{ Fill} = \left(\frac{M_i}{M_{full}} \right)$$

And

$$M_{full} = \text{Volume}_{gallons} * 0.9 * 0.45 * 3.78$$

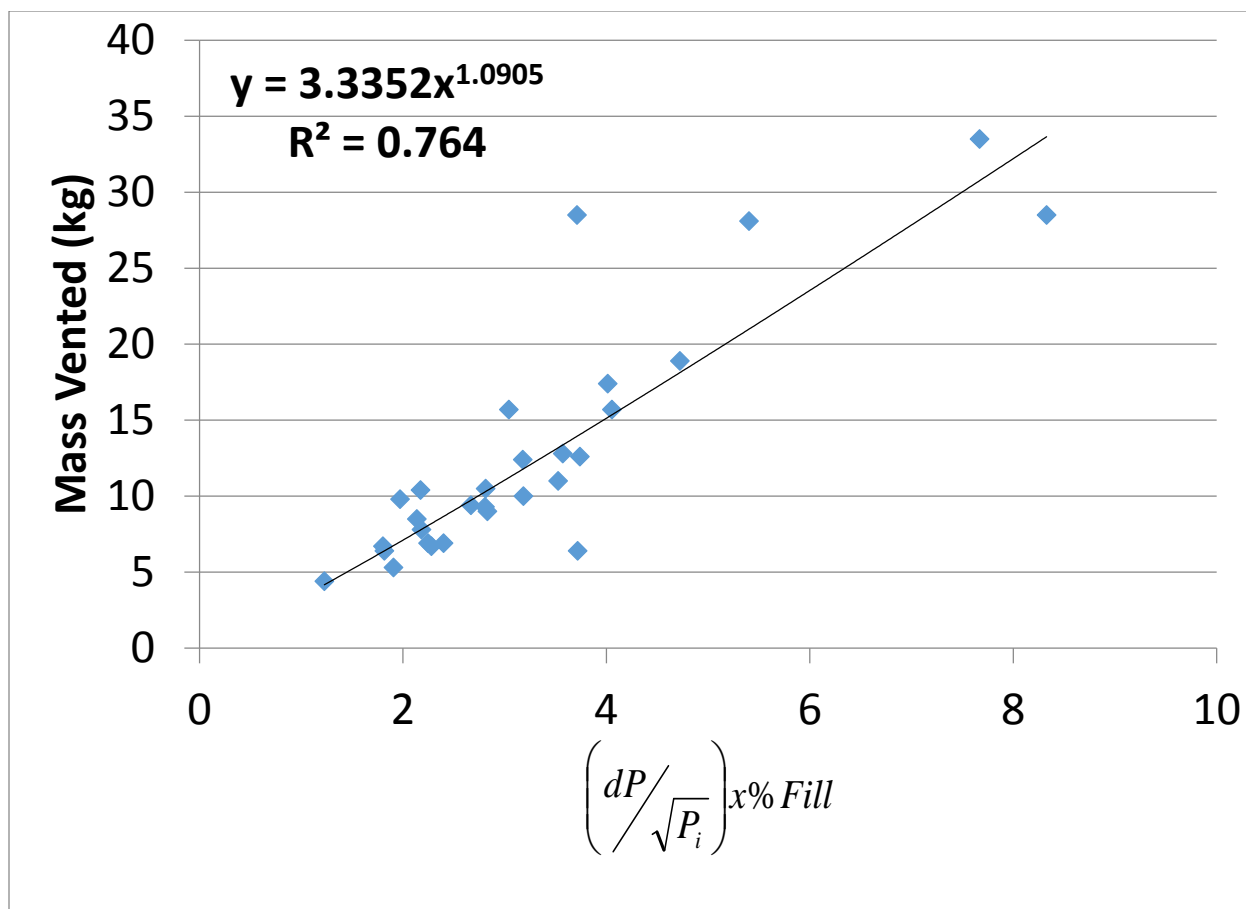


Figure S1-11: Mass vented as a function of pressures and fill level.

Additional Experimental Data and Analyses

A similar fit was done using the form $y=mx+b$ but this resulted in negative vent mass for small pressure changes (~10 psi). NorthStar LNG and Clean Energy conducted their own tank venting experiments. These experiments were similar to those performed at WVU in that the tank mass was continuously monitored and recorded during venting. These data were evaluated using the empirical equation developed from the WVU data and the vent mass from the equation and the actual measured values. It was noted that the WVU method to determine vented methane for a given pressure differential over-predicted the mass vented for these five cases by 7.2%.

By including these five additional data points to the WVU data set of 29 points, the new data set is shown in Figure S1-12. A separate least-squares regression was performed on a data set, which includes the WVU, Clean Energy/NorthStar, and Westport data. Figure 5 shows the revised empirical fit as compared to the Clean Energy/NorthStar and Westport data. Note that the error of the prediction decreased from 7.2% over-prediction to 4.5%.

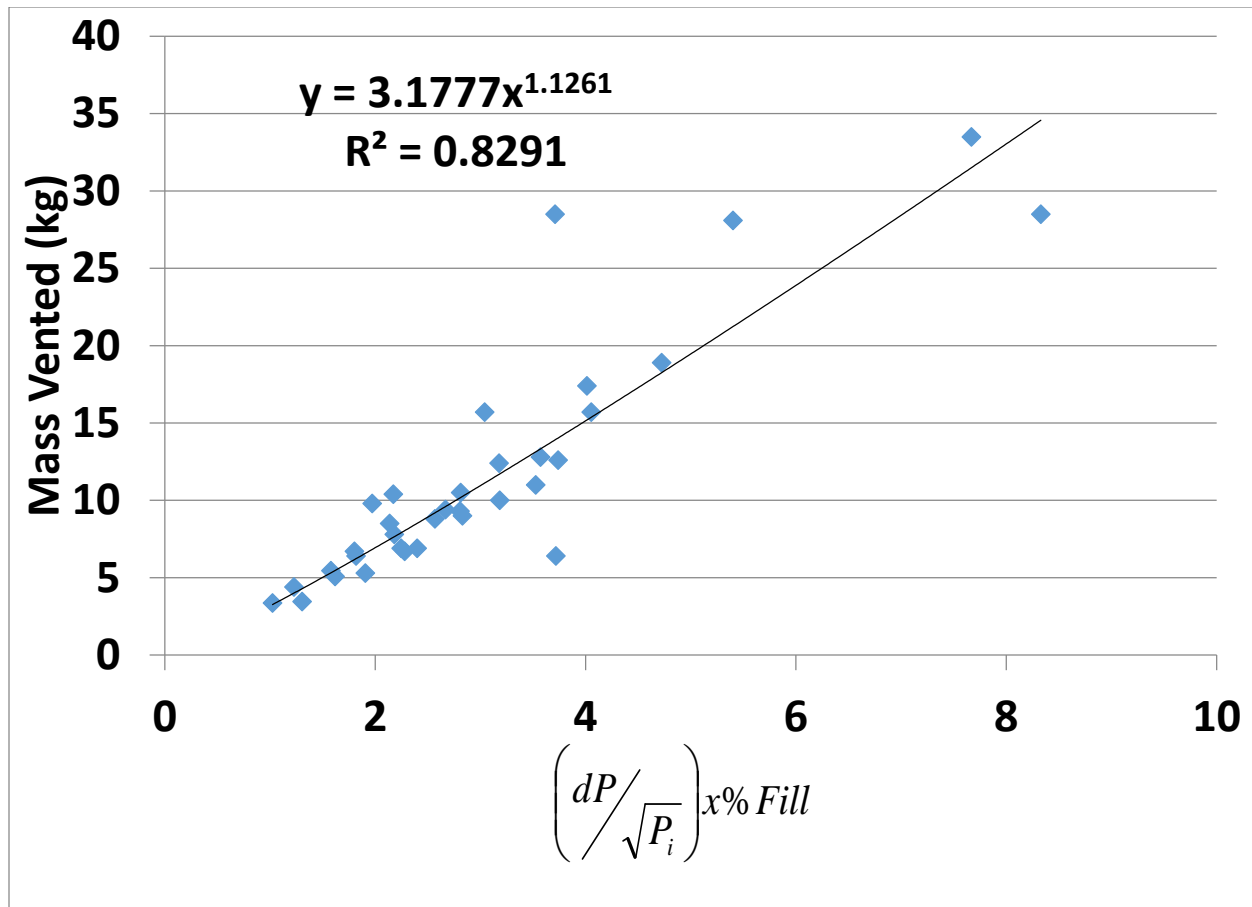


Figure S1-12: WVU data set and additional data points

- Mihai Ursan, "What is Boil-off?," LNG Task Force, Brussels, November 3, 2011.
http://www.unece.org/fileadmin/DAM/trans/doc/2011/wp29grpe/LNG_TF-02-09e.pdf
 Accessed: May 14, 2014. See worked examples in Appendix.

S1.4. CNG Stations

All of the CNG fueling facilities that participated in the study utilized the natural gas provided by pre-existing pipelines.

S1.4.1. CNG Station Configurations

There were three types of CNG station configurations: cascade fast-fill, buffer fast-fill, and time-fill.

A cascade fast fill station configuration was a system in which vehicles were primarily fueled from stored gas. These systems were typically employed in situations where fleets need to be fueled in short, peak periods. A cascade storage system normally consisted of three banks (storage vessels) of CNG stored at 4,200-4,600 psi. For vehicle refueling, dispensing begun with the lowest pressure storage reservoir and cycled through to the highest-pressure storage reservoirs based on pre-set flow rates to complete the fill. However, when refilling the station storage reservoirs the compressor would automatically switch on to fill the high-pressure reservoir first and then switched to the medium and low-pressure reservoirs. This was enacted to ensure that the high-pressure reservoir was maintained at maximum pressure at all times, thus guaranteeing that vehicles could be supplied with the maximum amount of fuel available.

During refueling in both types of fast fill stations, the pressure in the vehicle tank was monitored during delivery of the fuel. Based upon that measurement, the volume of the tank was calculated, in order to determine the amount of fuel needed to fill tank. After the tank was at capacity, the fuel flow was shut off.

A buffer fast-fill station configuration was a system in which vehicles were primarily fueled directly from compressors and employed a minimal amount of onsite storage in tanks. These systems were typically employed in situations where fleets required large volumes of fuel on a continuous basis or in a short of time. The buffer storage was utilized to allow the compressor(s) to continue to run loaded in between vehicle refueling. In this type of system, all filling reservoirs were connected and maintained at the same pressure at any instance in time.

A time-fill station configuration was a system in which vehicles were primarily fueled directly from compressors over a period of hours. These systems dispensed fuel through a fixed pressure regulator. When the fuel flow reaches a minimum rate, the fuel flow was shut off. Time-fill stations were typically employed in situations where fleets were on a structured schedule and returned daily to a central location, while out of service for many hours.

S1.4.2. CNG Station Leak Audit/Quantification Results

CNG Station No.1

CNG Station No.1 provided primarily slow-fill natural gas fueling to a fleet of 53 private commercial refuse vehicles that operated five days per week. It had the capability to provide both fast and slow fill to commercial vehicles. The facility was equipped with 60 time fill connections and two fast fill lanes. The fast fill lanes were the secondary fueling option and were primarily used for refueling vehicles mid-route or to fuel vehicles from other companies.

The fueling station system consists of two separate 4-stage compressors, a large desiccant dryer, auxiliary storage buffer tank, and an evacuation pump. The two, 4-stage compressors operated in parallel with a work rate dependent upon the current demand. The storage system utilized by this facility was of the buffer storage system type. The auxiliary storage tank was used as a buffer between the compressor and the vehicle to compensate for fluctuation in the compression process, for storage during an evacuation process (such as for maintenance), and provide additional fuel supply for fast fill vehicle refueling if needed. It had the capacity to hold enough CNG to fill about three refuse trucks in case of an emergency pump shutdown.

Due to multiple sources being in tight proximity and sheltered by a covering, the compressor unit was aggregated and treated as a single source for leak quantification using an enclosure. The compressor housing methane emissions were quantified while the compressor was on and off. The average emissions rates for one compressor were 3.15 and 19.4 grams per hour (g/hr), respectively. During the short-term audit, one leak was discovered and quantified with a leak rate of 0.88 g/hr. Refueling events were captured from six vehicles at the nozzle during disconnect only. The average refueling event measured during disconnect at the nozzle was 1.0 g/event.

CNG Station No.2

CNG Station No.2 was a private facility that provided fast-fill natural gas fueling to a fleet of 252 commercial transit vehicles that operated seven days a week. The facility was equipped with six fast fill dispensers on site. It was observed that only four fast fill dispenser stations were available for everyday use, with the other being available for emergency use (i.e. another CNG facility shuts down.) The storage system utilized by this facility was of the buffer storage system-type. During the 1st half of 2013 (1/1/2013-5/16/2013), this facility had a fuel throughput of approximately 827,154 DGE of natural gas, with the miles traveled by the fleet being 2,990,948.

The fueling station system consisted of three separate 4-stage compressors, air compressor, a large desiccant dryer, six auxiliary storage buffer tanks, two forced air ventilation systems, and an evacuation pump. Two of the compressors operate in parallel with a work rate dependent upon the current demand, with the other acting as an auxiliary. The compressors operated at 3800 psi and were powered by an electric motor. The compressors cycled on and off to match the fluctuation in gas demand. The site operator stated during typical operation that the compressors would cycle on- and off-line three to four times an hour after the buffer tanks and vehicles were filled. This facility used compressed air for all actuated valves.

During the short-term audit, 11 leak/loss sources were discovered and quantified, in addition to the compressor housing. The majority of the leak sources quantified was located on the compressor units contained inside the compressor housing. On the dryer unit, one leak of 3.6 g/hr was located on a gas regulator. Due to the moisture content in the natural gas at this facility, a minimum of one gallon of water was recovered from the dryer on a daily basis. The removal of the water from the dryer resulted in a small-unknown amount of gas to be released. This facility had two analyzers (moisture analyzer and gas chromatograph) that were designed to sample continuously and thus act as constant loss sources. The moisture analyzer was connected to the dryer system and determined when the system experienced a regeneration event to remove the moisture out of the natural gas. This moisture analyzer operates based on Faraday's Law of Electrolysis. According

to the moisture analyzer specifications, this particular model was supposed to vent constantly to the atmosphere at a rate of 1000scm. This would suggest a leak rate of approximately 43 g/hr. However, data collected on the moisture analyzer exhaust vent by WVU, resulted in an average leak rate of a 67.5 g/hr. The Gas Chromatograph was an analytical instrument that measured the content of various components in a sample. The natural gas sample was injected into the instrument where it entered a gas stream, which transported the sample into a separation chamber where various components were separated. The detector measured the various components as they exit the chamber. Typically, Helium or nitrogen was used as the carrier gas. This analyzer sampled continuously and thus can be considered a constant leak source at an average leak rate of 22.5 g/hr.

At this facility, the station was designed for the compressors to blowdown (depressurize) the gas left in the system to the atmosphere during the cycling from on to off. Unfortunately, WVU researchers were unable to capture any of these blowdown events due to time constraints imposed by facility site personnel. The compressor packing was also designed to be vented to the atmosphere through the blowdown vent pipe. The compressor packing for one compressor was 362 g/hr. The packing from the other two compressors were not measured due time constraints imposed by site personnel. The compressor units at this facility also had open crankcases that were vented to the atmosphere. The crankcase emissions from the compressors were not measured due safety concerns arising from the height of the vent.

Due to multiple sources being in tight proximity and enclosed by a covering, the compressor unit was aggregated and treated as a single source for leak quantification with an enclosure. The compressor housing methane emissions were quantified while the compressors were on and off. The average emissions rates for one compressor were 1515.7 and 376.9 grams per hour (g/hr), respectively. WVU researchers were able to identify several leaks on the compressor units, occurring at a pressure relief valve and flanges with the average leak rate being 12.5 g/hr.

The fueling dispensers at this facility were designed to vent to the atmosphere during every refueling event. WVU researchers were able to measure three refueling vent events. These refueling vent events had an average of 4.0 g/event. Unfortunately, WVU researchers were unable to capture any refueling events at the nozzle due to time constraints imposed by facility site personnel.

CNG Station No.3

CNG Station No.3 was a public facility that provided fast-fill natural gas fueling to heavy, medium, and light duty vehicles, seven days a week. The facility was equipped with four fast fill dispensers and eight fueling nozzles on site. However, it was observed that only seven fast fill fueling nozzles were available for use.

The fueling station system consisted of one 4-stage compressor, a large desiccant dryer, and three cascade-type storage tanks. The compressor was 400 hp with a max flow rate of approximately 800 scfm.

Due to multiple sources being in tight proximity and enclosed by a covering, the compressor unit was aggregated and treated as a single source for leak quantification using an enclosure. The

compressor housing methane emissions were quantified while the compressors were on and off. The average emissions rates for one compressor were 0 and 2.4 grams per hour (g/hr), respectively.

During the short-term audit, 12 leak locations were discovered and six leaks were quantified, in addition to the compressor housing. The continuous leaks measured were 41.3 g/hr. The largest leak (12.4 g/hr) at this facility occurred on the packing of an actuated valve. WVU researchers were unable to capture any refueling events due to lack of obtaining permission from vehicle owners.

CNG Station No.4

CNG Station No.4 was a public facility that provided fast-fill natural gas fueling to heavy, medium, and light duty vehicles, seven days a week. The facility was equipped with four fast fill dispensers and eight fueling nozzles on site.

The fueling station system consisted of three 4-stage compressors, a large desiccant dryer, and six cascade-type storage tanks. The storage tanks held approximately 90 DGE. The facility had an approximate fuel throughput per day of 1414 DGE. The actuated valves at this facility employed CNG as the operation fluid of choice. During the short-term audit, 15 leaks were discovered and five were quantified, in addition to the compressor housing. The average leak rate of the quantified continuous leak sources was 27.2 g/hr. The average leak rate of leaks associated with the dryer unit was 35.5 g/hr.

Due to multiple sources being in tight proximity and enclosed by a covering, the compressor unit was aggregated and treated as a single source for leak quantification using an enclosure. The compressor housing methane emissions were quantified while the compressors were on and off. The average emissions rates for one compressor were 19.1 and 6.7 grams per hour (g/hr), respectively. Refueling events were captured at the nozzle from four vehicles, with an average of 0.4 g/event. WVU researchers were unable to capture any refueling vent events due to the location of the vent.

CNG Station No.5

CNG Station No.5 was a private facility that provided fast fill natural gas fueling to 29 over-the-road tractor-trailers. The facility was equipped with two fast fill dispensers and four fueling nozzles on site.

The fueling station system consisted of three 4-stage compressors, a large desiccant dryer, and six cascade type storage tanks. Each compressor was rated at 800 scfm. The storage tanks held approximately 300 DGE total. This facility used CNG to operate the actuated valves on site. The pneumatic actuators on site were models 110 and 255. During the short-term audit, 33 leaks were discovered and 13 were quantified, in addition to the compressor housing. The average leak rate of the quantified continuous leak sources was 11.0 g/hr. The average leak rate of leaks associated with the dryer unit was 83.3 g/hr. During operation of the actuated valves at the priority panel, a transient loss rate of 165.5 g/hr was measured. However, for use in the estimation model an approximation for methane lost per operation of the pneumatic actuator was calculated. The amount of methane vented during the opening and closing of the model 110 actuator was 0.46 g

and 0.52 g, respectively. The amount of methane vented during the opening and closing of the model 255 actuator was 0.72 g and 1.00 g, respectively.

Due to multiple sources being in tight proximity and environed by a covering, the compressor unit was aggregated and treated as a single source for leak quantification using an enclosure. The compressor housing methane emissions were quantified while the compressors were on and off. The average emissions rates for one compressor were 279.0 and 0.8 grams per hour (g/hr), respectively. Refueling events were captured from three vehicles at the nozzle, with an average of 0.3 g/event. WVU researchers were unable to capture any refueling vent events due to the location of the vent.

CNG Station No.6

CNG Station No.6 was a private facility that provided fast-fill natural gas fueling to 61 transit vehicles that operated five days a week on a full schedule, and two days on a modified schedule. The facility was equipped with one fast fill dispenser and two fueling nozzles on site.

The fueling station system consisted of three, 4-stage compressors, a large desiccant dryer, and 12 cascade type storage tanks. Two of the compressors operated in parallel with a work rate dependent upon the current demand, with the other acting as an auxiliary. The actuated values at this facility operated with compressed air. During the short-term audit, 29 leaks were discovered and 11 were quantified, in addition to the compressor housing. The average leak rate of the quantified continuous leak sources was 67.8 g/hr. The average leak rate of leaks associate with the dryer unit was 0 g/hr. The compressor units were measured without the use of an enclosure. The compressor housing methane emissions were quantified while the compressors were on and off. The average emissions rates for one compressor were 1086.6 and 4.8 grams per hour (g/hr), respectively. The compressor units had packing vented to the atmosphere. The packing leak from one compressor was 448 g/hr. The other compressor-packing leak over ranged the HVS system, meaning the leak exceeded 1.4 kg/hr. Refueling events from the nozzle were captured from five vehicles, with an average of 0.8 g/event. Refueling events from the vent were captured from eight vehicles, with an average of 2.5 g/event.

CNG Station No.7

CNG Station No.7 was a public facility that provided fast-fill natural gas fueling to heavy, medium, and light duty vehicles, seven days a week. The facility was the CNG portion of a LCNG facility. To produce CNG, the LNG was pumped into a vaporizer that converts it from liquid to gas. The site was equipped with one fast fill dispenser. The CNG portion consisted of one compressor, an odorant system, and three cascade type storage tanks.

During the short-term audit, nine leaks were discovered and two were quantified, in addition to the compressor housing. The average leak rate of the quantified continuous leak sources was 0.6 g/hr. The compressor units were measured without the use of an enclosure. The compressor housing methane emissions were quantified while the compressors were on and off. The average emissions rates for one compressor were 0 and 1.5 grams per hour (g/hr), respectively. Refueling events from the nozzle were captured from five vehicles, with an average of 0.1 g/event. Refueling events from the vent were unable to be captured due to the location of the vent.

CNG Station No.8

CNG Station No.8 was a private facility that provided fast-fill natural gas fueling to 27 over-the-road tractor-trailers. The facility was equipped with two fast fill dispensers on site.

The fueling station system consisted of three 4-stage compressors, a large desiccant dryer, and four buffer type storage tanks. Two buffer storage reservoir tanks were connected in parallel and associated with one fueling dispenser. The large three 4-stage compressors were capable of delivering more than 11 gallons of CNG per minute. The facility operated actuated valves with CNG. During the short-term audit, 19 leaks were discovered and quantified, in addition to the compressor housing. The average leak rate of the quantified continuous leak sources was 33.2 g/hr. The average leak rate of leaks associated with the dryer unit was 0 g/hr. Due to multiple sources being in tight proximity and enveloped by a covering, the compressor unit was aggregated and treated as a single source for leak quantification using an enclosure. The compressor housing methane emissions were quantified while the compressors were on and off. The average emissions rates for one compressor were 11.3 and 1.6 grams per hour (g/hr), respectively. Refueling events from the nozzle were measured from three vehicles, with the average being 0.2 g/event. Refueling events from the vent were measured from three vehicles, with the average being 4.0 g/event.

S1.4.3. CNG Vehicle Refueling

For the CNG stations visited, the refueling process procedures differed depending upon the nozzle design. Typically, the nozzle was connected by turning or squeezing a lever to make the attachment, or an action similar to a quick disconnect. Once the nozzle was attached, the lever on the pump was turned to the START position to begin the fill. The electronic controller automatically measured the temperature and pressure, and monitored the flow rate during the fill. When the temperature-adjusted fill pressure was reached, the controller automatically terminated the refueling process. As soon as the fill was completed, the gas (pressure) left in the hose system was released to the atmosphere through a second hose connected to the nozzle and typically ran above the fueling canopy. For this study, the amount of gas released during this process was referred to as refueling vent. The lever on the pump was turned to STOP and the nozzle was detached from the vehicle releasing a small amount of CNG. For time fill stations, CNG dispensers or fill posts support multiple hoses. Each hose has a nozzle and a shut-off valve. To fuel, a hose was connected to the vehicle, the valve was turned on, and the tanks slowly fill over an extended period. After the vehicle was filled, the lever on the pump was turned to STOP and the nozzle was detached from the vehicle releasing a small amount of CNG, equivalent to the dead space volume associated with the nozzle.

CNG refueling events were captured from 36 heavy-duty vehicles, 22 were measured at the nozzle, and 14 were measured at the vent. The summary of refueling events can be seen in Figure S1-13 and Figure S1-14.

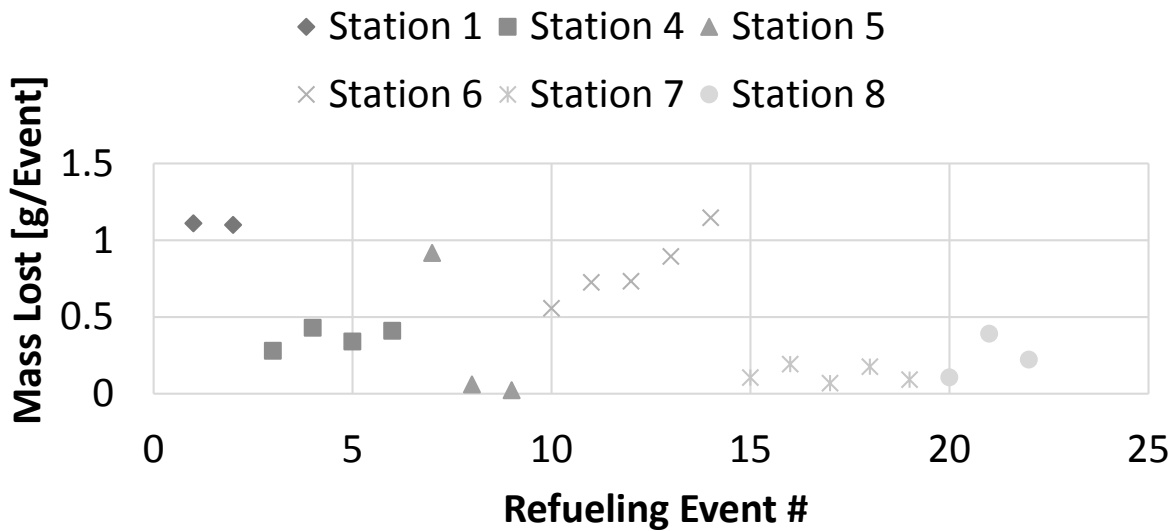


Figure S1-13: CNG refueling events at nozzle

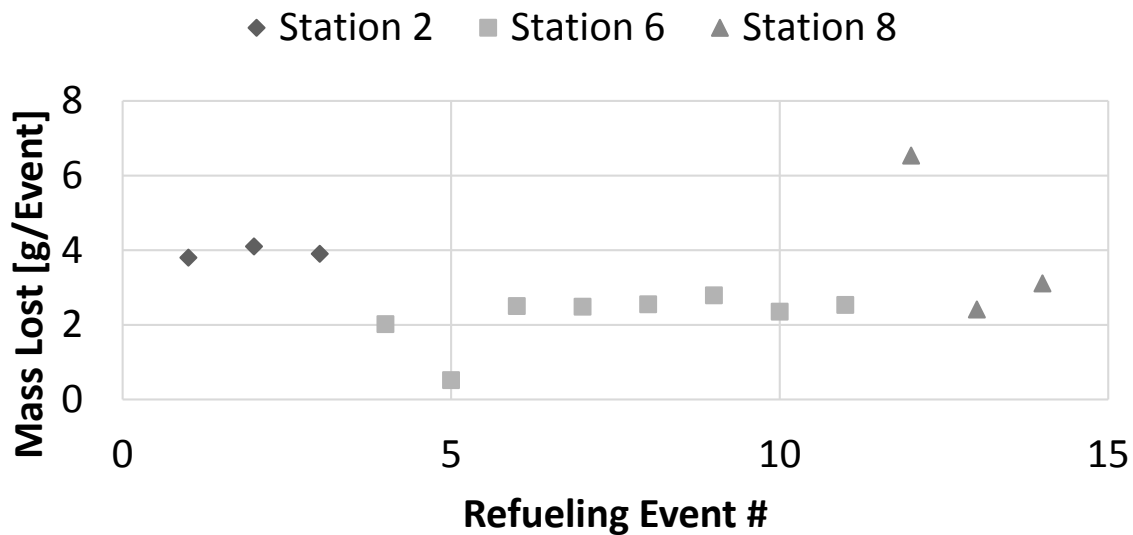


Figure S1-14: CNG refueling events at vent

The minimum, maximum, and average values occurring at the nozzle were respectively, 0.02, 1.14, and 0.46 g/event. The minimum, maximum, and average values occurring at the vent were respectively, 0.51, 6.54, and 2.97 g/event

S1.4.4. Compressor Losses

The compressors utilized at a CNG refueling facility contain both leak and loss components. The Fugitive emissions stemming from leaks occur typically at normally sealed components on the pressurized piping and equipment systems. Those components can include flanges, screwed fittings, pressure relief valves (PRV), valve seats, seals, etc. The fugitive emissions stemming

from loss components can occur at the valve stem packing, packing rods, crankcase, blowdown vents, etc. Figure S1-15 displays an example of a typical natural compressor.

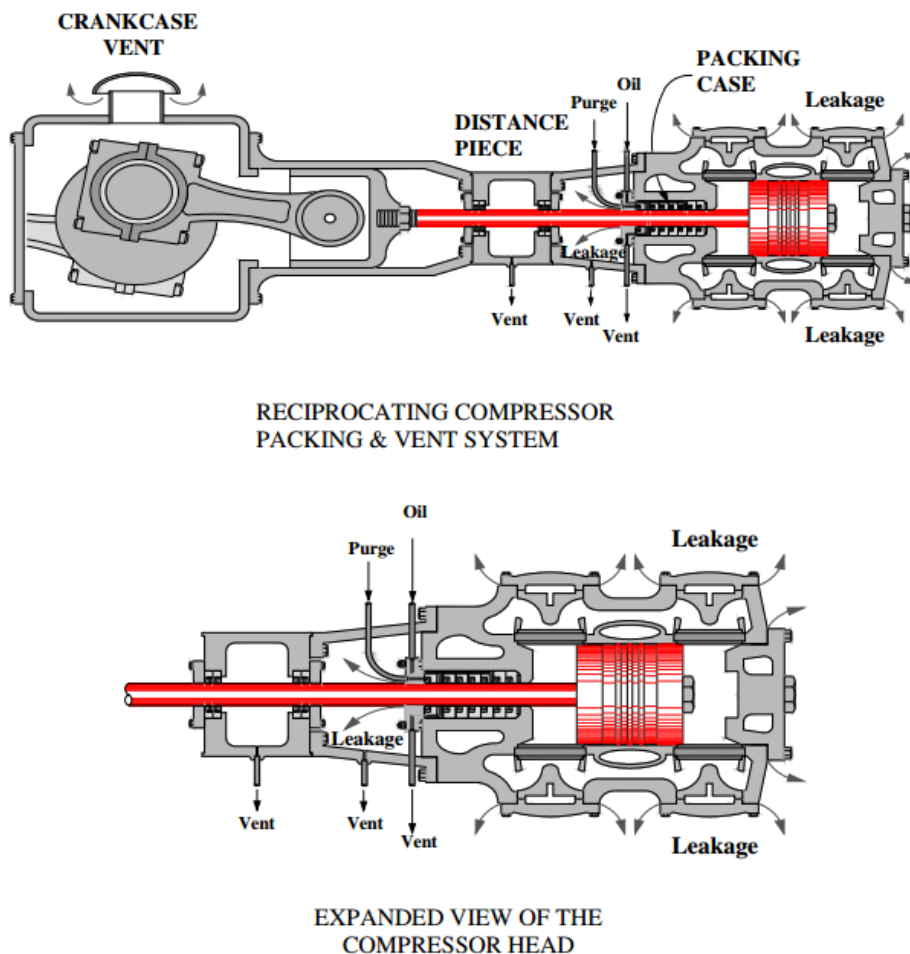


Figure S1-15: Natural gas compressor schematic (Picard, Ross, & Smith, 2002)

Compressor Packing

The compressor packing refers to the seal around the reciprocating rod of the compressor. The main purpose of this seal was to prevent leakage of natural gas between a cylinder and a piston rod. The amount of leakage increases as the clearance increases, and relatively decreases as the speed of the compressor increases.

Blowdown

There currently exist several variations in station design, for when compressors at CNG refueling stations were taken offline for maintenance or shut down during typical operation. During the short-term audit portion of this study, WVU personnel observed three different design strategies employed when a compressor shuts down.

In one design, the high-pressure gas remaining within the compressors and associated piping between isolation valves was vented to the atmosphere ('blowdown'), anytime the compressors were shut down.

In the other two designs, the facilities employed a blowdown recovery, in which no methane was intentionally released into the atmosphere during the cycling of the compressor units. In the second design, the blowdown vent line of the compressor was routed to a storage tank, recovering all, of the vented gas. The gas accumulated in the storage tank was recompressed by the system automatically. The third system design encountered was able to reduce methane emissions associated with the compressor cycling by keeping the systems fully or partially pressurized during the shutdown.

It was important to note, that both a pressurized and depressurized system may leak. For example, the pressurized system may leak from a closed blowdown valve, reciprocating compressor rod packing, etc. A depressurized system may continue to leak from a defective or improperly sealed unit isolation valve.

Compressor Vent

During the audit portion of the study, WVU personnel observed that many CNG refueling station compressor units contained vents opened to the atmosphere that originated from the compressor units. The vents were installed as a safety measure, meaning any release of methane through the vents would be unintentional, and the result of a component failure or malfunction.

Priority Panel

The priority panel was a valve panel that directs the CNG flow from the compressor(s) on-site storage or directly to the vehicle. Some facilities also have a sequential panel that directs the flow of CNG from the compressor or tanks to fuel disperser units. This panel also insures temperature compensated fills. The priority panel manages the storage filling sequence, typically giving priority to the high-pressure storage vessels filling in order to ensure vehicle tanks were refueled at the highest pressure. For buffer type facilities, the panels direct flow to a fuel dispenser or to storage vessels that were together in a manifold. For cascade type systems, the three-bank priority panel directs flow to one of three groups of vessels and some facilities had the direct fill capability to direct flow to the dispensers. For the cascade type system, there was one actuator for every storage vessel and dispenser on site.

The actuated valves can be operated using with CNG or compressed air. One facility audited during the course of the study employed natural gas to operate the pneumatic actuators on site. The pneumatic actuators on site were models 110 and 255. In order to estimate correctly the amount of methane dispensed during actuation of the pneumatic valve the specifications shown in Figure S1-16 were used in conjunction with Equation S1-.

Model	Air Volume Opening (L)	Air Volume Closing (L)	Air Volume Opening (Cu.In.)	Air Volume Closing (Cu.In.)
020	0.12	0.16	7	10
035	0.21	0.23	13	14
050	0.3	0.34	18	21
075	0.43	0.47	26	29
110	0.64	0.73	39	45
160	0.95	0.88	58	54
255	1	1.4	61	85
400	2.5	2.2	153	134
500	3.7	3.2	226	195
550	5.9	5.4	360	329
600	7.5	7.5	458	458
650	11	9	671	549
700	17	14	1037	854

Figure S-16: Aero2 Pneumatic Actuators Performance Data during operation

The volume of air associated with the opening and closing of the valve was transformed to mass of methane vented per event through the application of Equation S1-4.

$$CH_4[g] = (Air\ L) \left(\frac{1\ mole}{22.4\ L} \right) \left(\frac{16.04\ g\ CH_4}{1\ mole\ CH_4} \right) \quad \text{Equation S1-4}$$

The amount of methane vented during the opening and closing of the model 110 actuator was 0.46 g and 0.52 g, respectively. The amount of methane vented during the opening and closing of the model 255 actuator was 0.72 g and 1.00 g, respectively.

Several of the stations visited did not have isolation valves provided on the underground lines. If maintenance were required in the panel for these facilities, all underground lines would have to be completely depressurized. This has the potential to release a significant quantity of gas, although WVU researchers did not observe this action. Other facilities audited during the campaign, employed either isolation valves or mounted “U” shaped tube assemblies around the valves requires frequent service. This allows for their removal without the need to disassemble adjacent tubing.

S1.4.5. CNG Station Summary Results

The results of CNG short-term station audits have been aggregated to form a summary suitable for use in the estimation model, shown in Table S1-10. The continuous emissions contains emissions that occur 24 hours a day, this includes those that occur from intentional design (i.e. vents from analyzers) and those occurring from the malfunction of components (i.e. leaks). The compressor emissions associated with the operation of the compressor or compressor “ON” includes emissions measured during the operation of the compressor, compressor packing, the dryer, and the compressor vent. The compressor emissions associated with compressor “OFF” includes emissions measured from the compressor when the unit was not running.

Table S1-10. CNG Station Audit Result Summary

Station	Continuous emissions [g/hr]	Compressor	
		ON [g/hr]	OFF [g/hr]
1	0.9	3.2	19.4
2	90.0	1519.7	376.9
3	41.3	0.0	2.4
4	40.7	55.1	6.7
5	11.0	421.6	0.8
6	67.8	1087.6	4.8
7	0.6	0.0	1.5
8	33.2	16.9	1.6
Average	35.7	388.0	51.8

The measurements obtained for the dead space volume of the nozzle and vent during vehicle refueling were aggregated to get a single value associated with vehicle refueling. The minimum, maximum, and average values occurring at the nozzle were respectively, 0.02, 1.14, and 0.46 g/event. The minimum, maximum, and average values occurring at the vent were respectively, 0.51, 6.54, and 2.97 g/event. The aggregated average value of a CNG vehicle refueling was 3.43.

S1.4.6. General CNG Station Observations

- The compressor blowdown to atmosphere station design was seen at one station.
- The station design of venting the compressor packing to the atmosphere was seen at two stations.
- Continuously sampling analyzers were located at one station.
- A cascade type storage system was seen at five stations.
- A buffer type storage system was seen at three stations.
- A refueling nozzle design in which methane was intentionally released through a vent was seen at seven stations.
- A recovery system was utilized by seven of the stations.

S1.5. Vehicle Performance and Engine Related Methane Emissions Data

Tailpipe and crankcase data were collected from twenty-two vehicles. Vehicles included transit buses and refuse trucks powered by stoichiometric natural gas engines and over-the-road (OTR) tractors powered by stoichiometric natural gas engines, high-pressure direct injection diesel/natural gas engines, and diesel engines retrofitted with kits allowing for dual-fuel diesel-natural gas operation. The stoichiometric natural gas engines in the OTR tractors included both 9 and 12-liter engines.

S1.5.1. Data Processing

Introduction

Data from testing on a chassis dynamometer and on-road were processed into microtrips and categorized based on average non-idle speed. The fuel energy was based on carbon in the vehicle exhaust while tailpipe methane was based on direct exhaust measurements. Specific fuel energies used to convert fuel mass to fuel energy were 47.141 MJ/kg for CNG, 48.632 MJ/kg for LNG, and 42.612 MJ/kg for diesel fuel. Crankcase methane was either measured directly during chassis dynamometer testing (separate from tailpipe methane) when available or modeled based on engine boost pressure.

Data Processing Methodology

Total powertrain methane emissions were available from a portion of the chassis and on-road tests performed. In the case of chassis testing, separate measurement systems were employed to measure tailpipe and crankcase methane emissions, which were later combined to calculate engine related methane emissions. For on-road tests, the vehicle crankcase vent was routed to the exhaust such that a combined tailpipe+crankcase vent measurement was obtained. Tailpipe only methane emissions were available for all of the chassis tests and for some on-road tests where the crankcase vent was not routed with the exhaust. For chassis and on-road tests performed before crankcase vent emissions were included in the characterization, a model based on engine boost pressure was used to estimate crankcase vent emissions.

S1.5.2. Microtrip Averaged Results

A non-idle microtrip was defined as a portion of a tested cycle where the vehicle speed starts at zero (idle), accelerates to a higher speed, travels an indeterminate distance, and decelerates to zero (idle). The non-idle microtrip was followed by an idle microtrip. An idle microtrip maintained idle speed until the next non-idle microtrip began. The idle microtrips were excluded from the analysis in this document.

The following figures present tailpipe and vent emissions on a fuel specific basis and fuel economy against average non-idle microtrip speed for each engine group examined. Data for individual microtrips from each category subsequently averaged to arrive at input parameters for use in scenarios and the estimation model. Note that data from microtrips where tailpipe and crankcase emissions were measured separately were included in both the tailpipe and total emissions figures while data from microtrips where only tailpipe methane or where mixed tailpipe and crankcase methane were measured only appear in a single respective chart.

S1.5.3. Vehicles with 9 Liter Stoichiometric NG Engines

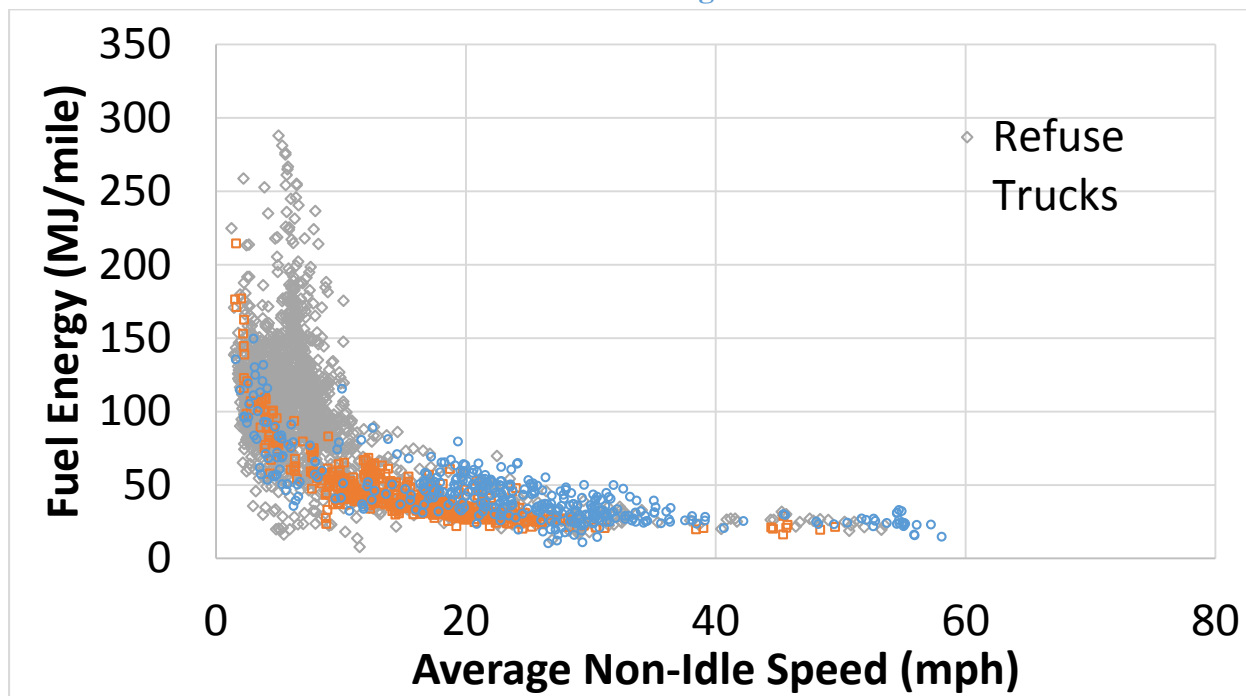


Figure S1-2: Fuel energy vs average non-idle speed for all 9-liter stoichiometric engine powered vehicles. (n=2902)

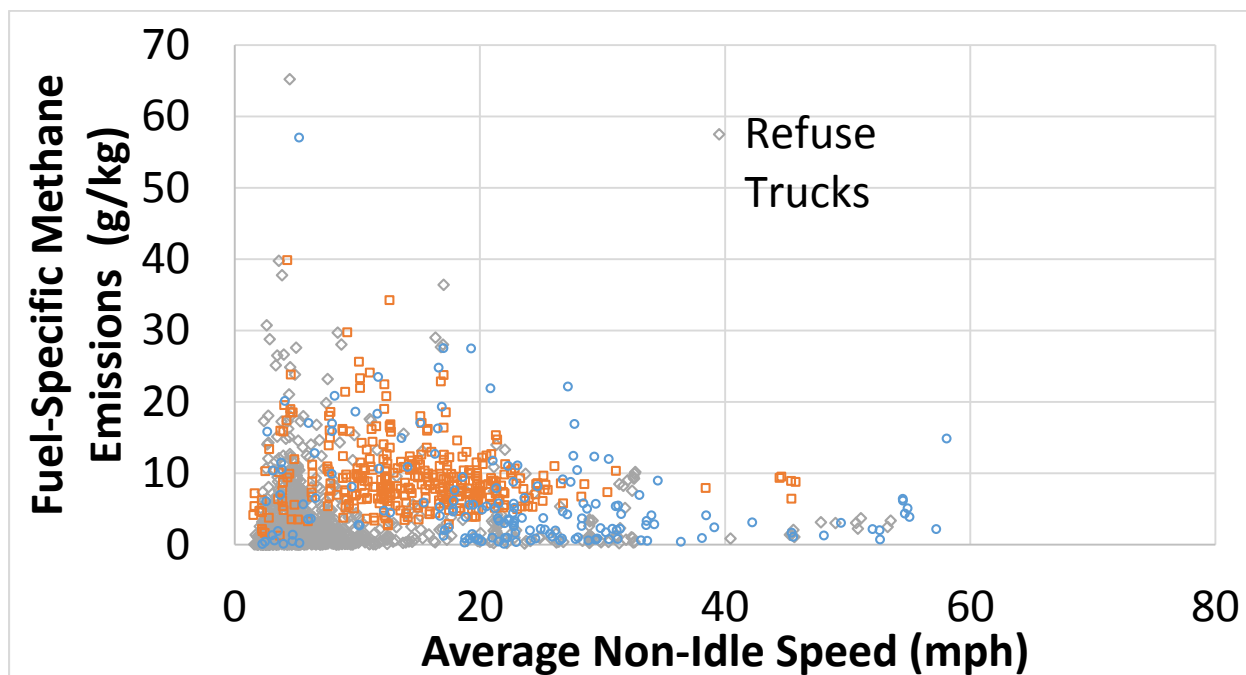


Figure S1-18: Fuel-specific tailpipe methane emissions vs average non-idle speed for all 9-liter stoichiometric NG engine powered vehicles. (n=1711)

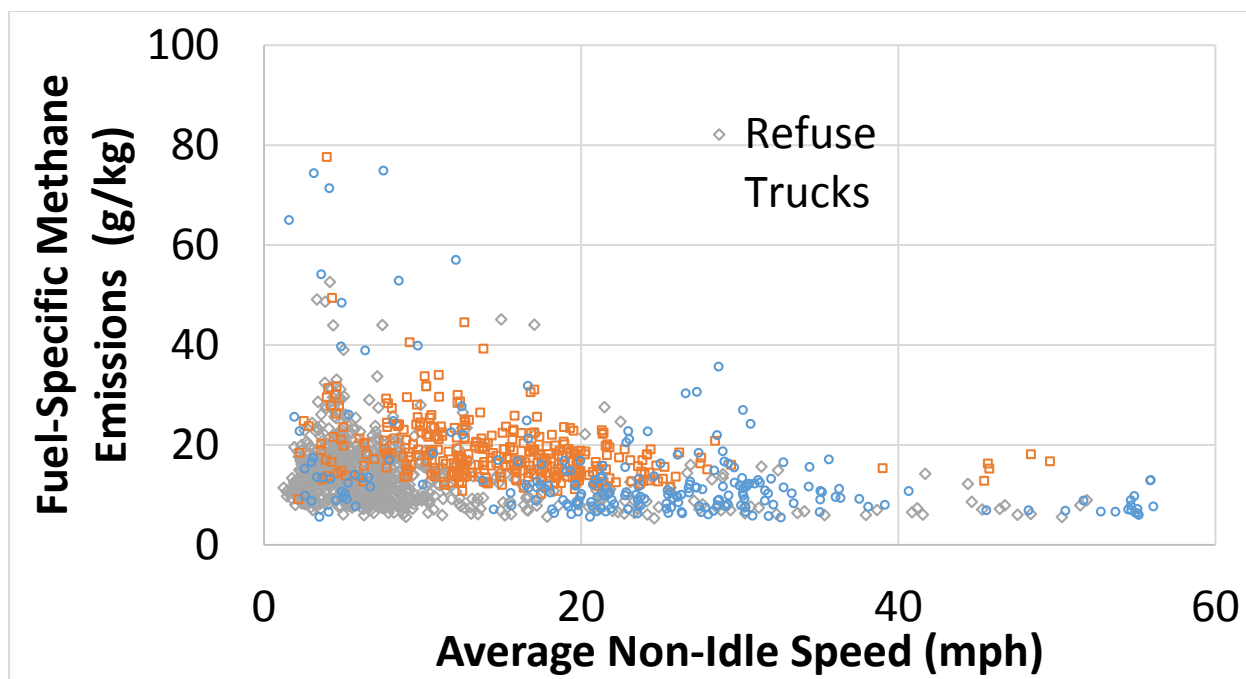


Figure S1-39: Fuel-specific total (including tailpipe and crankcase) methane emissions vs average non-idle speed for all 9 Liter engine powered vehicles (n=1482)

S1.5.4. OTR Tractors with 9 Liter Stoichiometric NG Engines

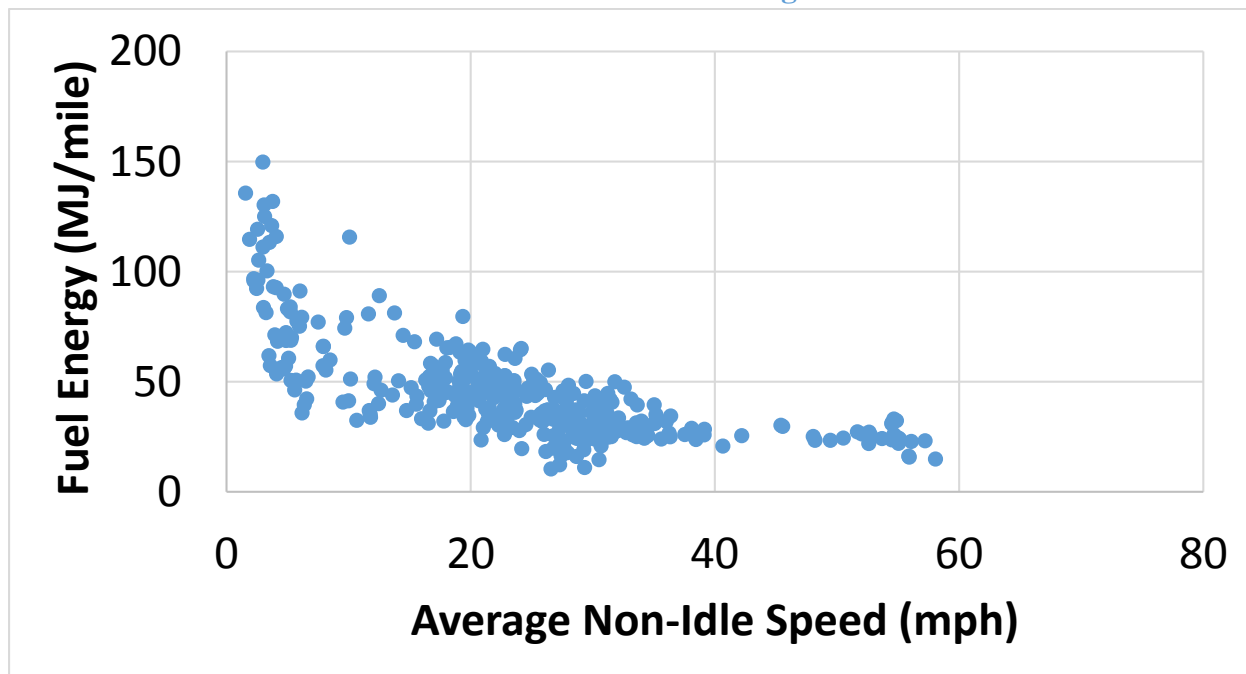


Figure S1-20: Fuel energy vs average non-idle speed for all 9-liter stoichiometric engine powered OTR tractors. (n=376)

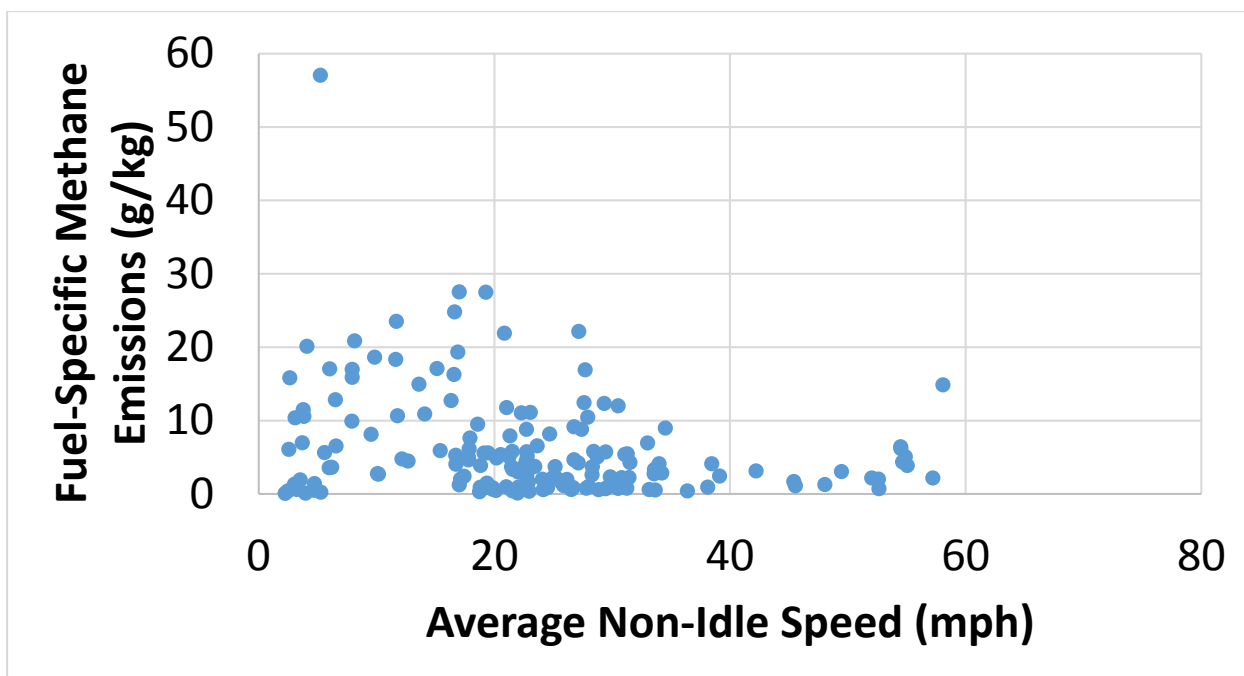


Figure S1-21: Fuel-specific tailpipe methane emissions vs average non-idle speed for all 9-liter stoichiometric NG engine powered OTR tractors. (n=167)

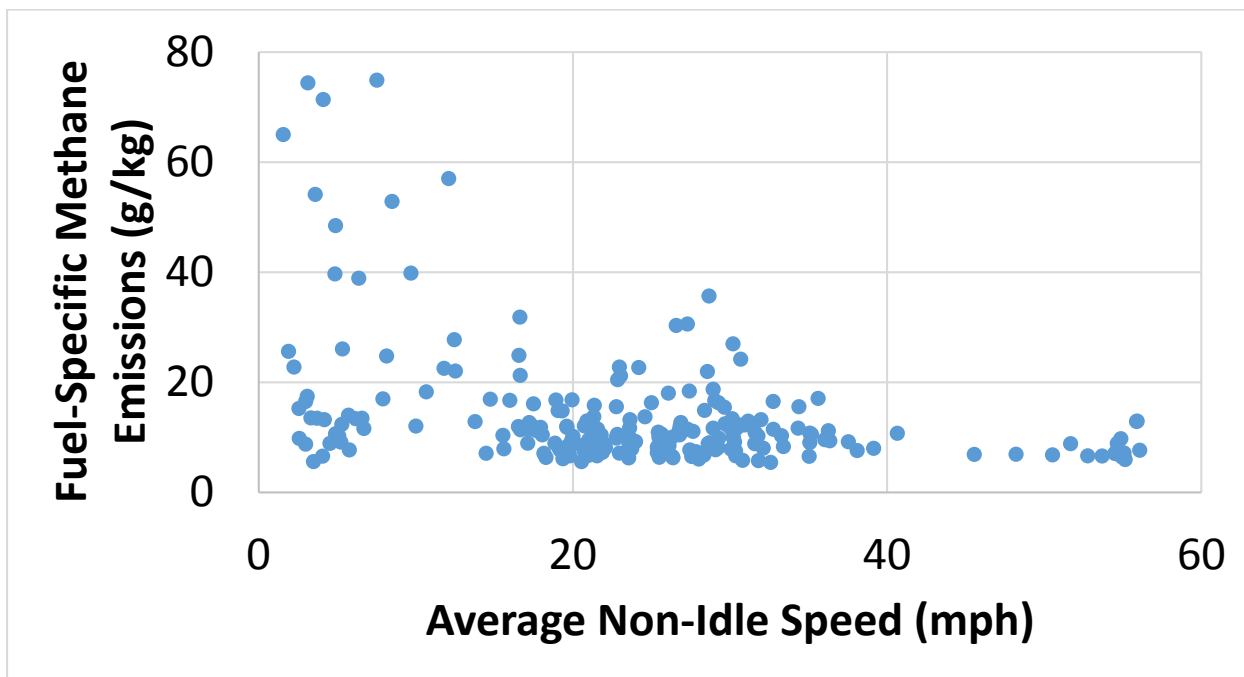


Figure S1-22: Fuel-specific total (including tailpipe and crankcase) methane emissions vs average non-idle speed for all 9 Liter engine powered OTR Tractors (n=225)

S1.5.5. OTR Tractors with 12 Liter Stoichiometric NG Engines

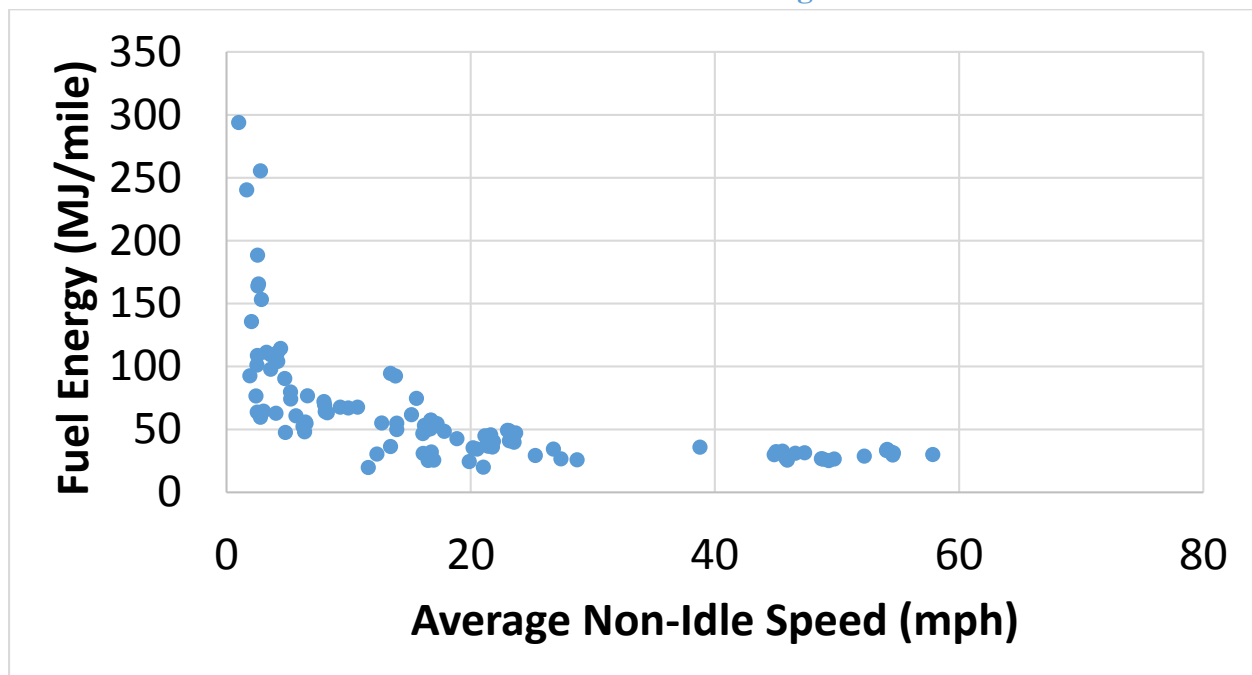


Figure S1-23: Fuel energy vs average non-idle speed for all 12 liter stoichiometric engine powered OTR tractors (n=106)

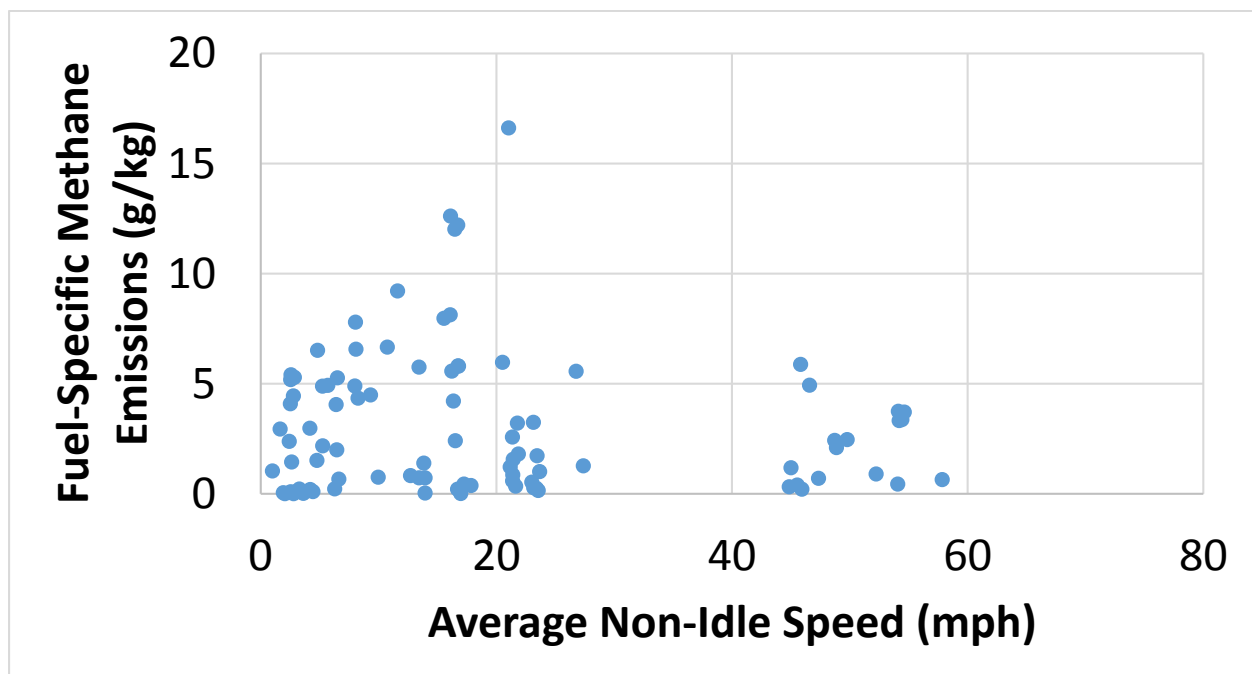


Figure S1-24: Fuel-specific tailpipe methane emissions vs average non-idle speed for all 12-liter stoichiometric NG engine powered OTR tractors. (n=93)

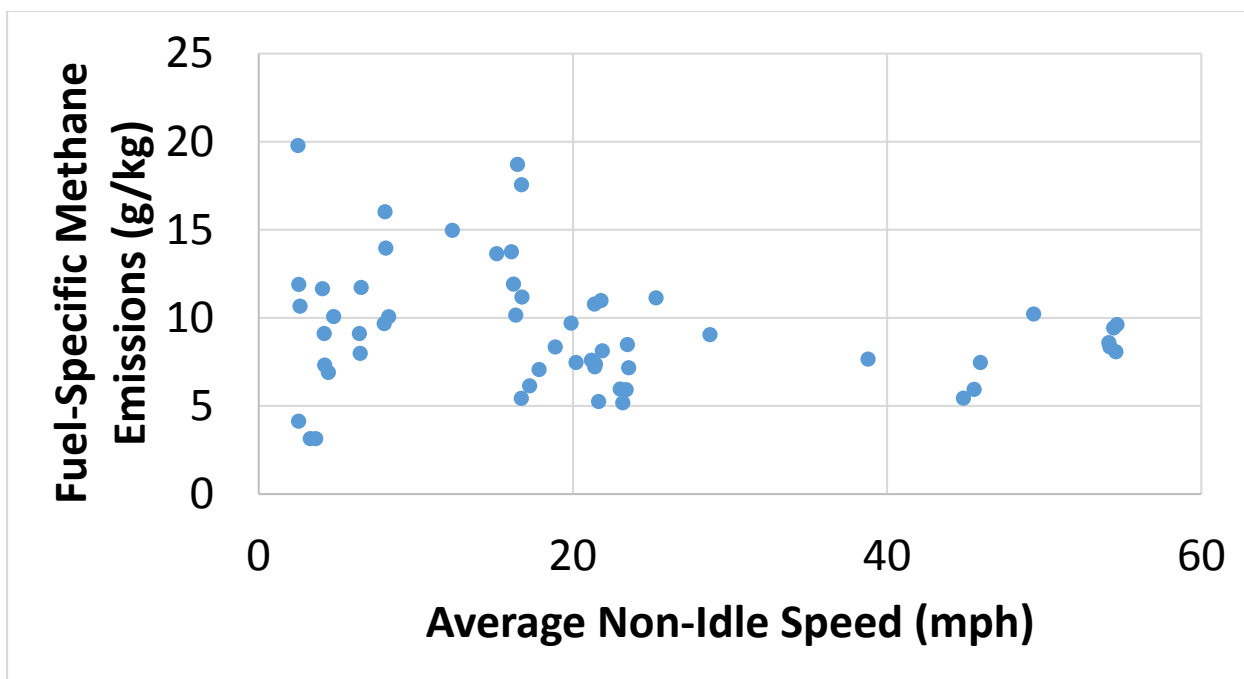


Figure S1-25: Fuel-specific total (including tailpipe and crankcase) methane emissions vs average non-idle speed for all 12 Liter stoichiometric NG engine powered OTR tractors (n=56)

S1.5.6. OTR Tractors with HPDI Engines

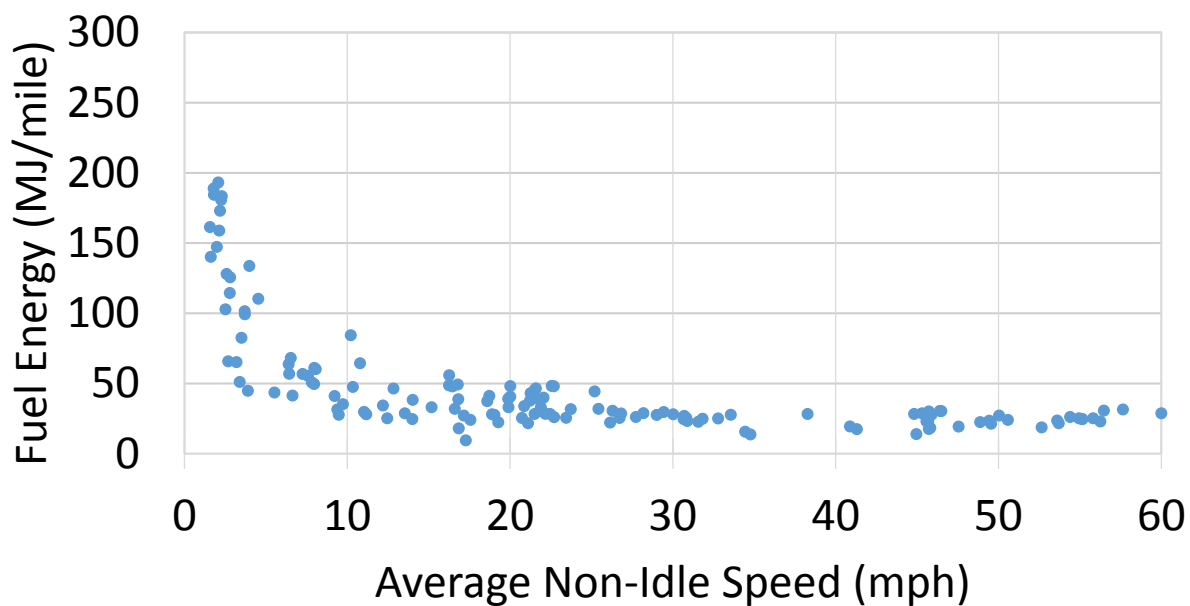


Figure S1-26: Fuel energy vs average non-idle speed for all HPDI engine powered vehicles (n=142)

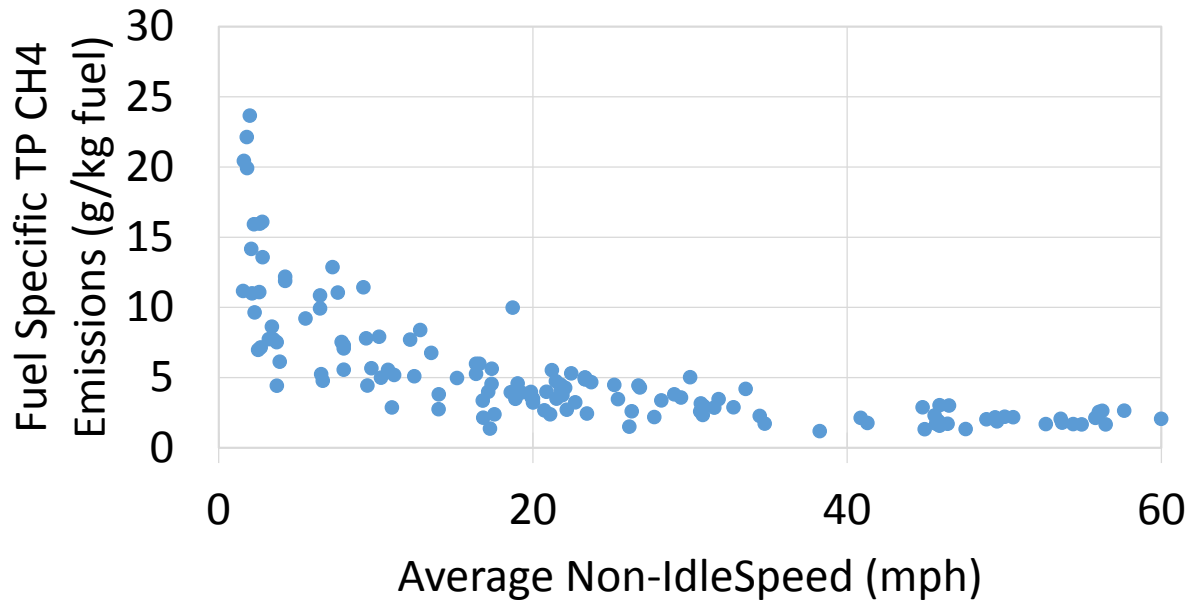


Figure S1-27: Fuel-specific tailpipe methane emissions vs average non-idle speed for all HPDI engine powered vehicles (n=142)

S1.5.7. Final Processed Vehicle Data

The driving schedules for each vehicle were divided into idle and non-idle microtrips. A non-idle microtrip was defined as a portion of a tested cycle where the vehicle speed starts at zero mph, accelerates to a higher speed, travels an indeterminate distance, and decelerates to zero mph. The non-idle microtrip was followed by an idle microtrip. An idle microtrip maintains idle speed until the next non-idle microtrip begins. Sensors inherently have noise and can register small velocity measurements, even when the vehicle was stationary. False microtrips can develop out of this noise. Therefore, a filter was applied to eliminate the false microtrips. If the maximum speed of a microtrip was less than 3.6 mph and the duration of the microtrip was less than 5 seconds, the velocity of the entire microtrip was set to zero.

The non-idle microtrips were sorted to city, arterial, and highway activities by the average velocity, as shown in Table S1-11. An average velocity of 0.2 mph was used as an upper bound for the idle activity as a redundant filter for the sensor noise removal.

Table S1-11: Bins of Average Speed for Each Activity

Activity	Bin of Average Speed (mph)
Idle	[0,0.2]
City	(0.2,10]
Arterial	(10,40]
Highway	>40

All of the microtrips in the same bin were added together consecutively to create activities for each vehicle. For example, all microtrips from vehicle 3 with an average speed between 0.2 mph and 10 mph were added consecutively to make one set of data with multiple microtrips, or a city activity for vehicle 3. The fuel specific tailpipe and crankcase emissions and the mile specific fuel energy for the transit buses, refuse trucks, 9 liter SI OTR tractor, 12 liter SI OTR tractor, and the 15 liter HPDI OTR tractor are shown in Table S1-12, Table S1-13, Table S1-14, Table S1-15, Table S1-16, respectively.

Table S1-12: Tailpipe and crankcase emissions and for three stoichiometric 9L transit buses

	Vehicle	Idle	City	Arterial	Highway	Test Methods
Tailpipe Methane (g/kg fuel)	Vehicle A (V14)	2.08	10.48	8.54	6.42	Chassis Only
	Vehicle B (V15)	3.67	10.21	8.92	8.87	Chassis/On-Road
	Vehicle C (V16)	5.80	10.01	9.53	9.43	On-Road Only
	Average	3.85	10.23	9.00	8.24	N.A.
Crankcase Methane (g/kg fuel)	Vehicle A (V14)	14.09	10.04	7.94	6.38	Chassis Only
	Vehicle B (V15)	13.01	9.38	7.88	6.74	Chassis/On-Road
	Vehicle C (V16)	11.34	11.72	8.19	6.64	On-Road Only
	Average	12.81	10.38	8.00	6.63	N.A.
Fuel Energy (MJ/mile) *Idle (MJ/hr)	Vehicle A (V14)	259.12*	64.77	43.70	28.73	Chassis Only
	Vehicle B (V15)	256.62*	58.87	30.97	18.33	Chassis/On-Road
	Vehicle C (V16)	321.19*	44.87	30.58	20.76	On-Road Only
	Average	278.98*	56.03	35.08	22.61	N.A.

Table S1-13: Tailpipe and crankcase emissions and dsfc for five 9L stoichiometric refuse trucks

	Vehicle	Idle	City	Arterial	Highway	Test Methods
Tailpipe Methane (g/kg fuel)	Vehicle A (V6)	0.32	3.70	9.79	2.05	Chassis Only
	Vehicle B (V7)	1.15	4.96	4.26	2.82	Chassis/On-Road
	Vehicle C (V13)	0.39	2.03	1.56	3.04	On-Road Only
	Vehicle D (V5)	0.88	2.63	9.00	1.08	Chassis Only
	Vehicle E (V12)	0.61	1.62	2.36	2.03	On-Road Only
	Average	0.67	2.99	5.39	2.20	N.A.
Crankcase Methane (g/kg fuel)	Vehicle A (V6)	20.93	8.12	6.99	5.41	Chassis Only
	Vehicle B (V7)	18.06	10.54	7.89	5.64	Chassis/On-Road
	Vehicle C (V13)	14.99	9.07	7.55	5.75	On-Road Only
	Vehicle D (V5)	19.08	9.13	7.17	5.37	Chassis Only
	Vehicle E (V12)	10.41	8.42	7.37	5.62	On-Road Only
	Average	16.62	9.06	7.39	5.56	N.A.
Fuel energy (MJ/mile) *Idle (MJ/hr)	Vehicle A (V6)	186.97*	103.88	37.10	29.16	Chassis Only
	Vehicle B (V7)	195.91*	81.22	31.42	24.71	Chassis/On-Road
	Vehicle C (V13)	249.62*	82.30	33.38	18.82	On-Road Only
	Vehicle D (V5)	197.31*	98.35	34.58	29.97	Chassis Only
	Vehicle E (V12)	349.77*	199.19	35.67	19.75	On-Road Only
	Average	235.92*	112.99	34.43	24.48	N.A.

Table S1-14: Tailpipe and crankcase emissions and dsfc for three 9L stoichiometric OTR tractors

	Vehicle	Idle	City	Arterial	Highway	Test Methods
Tailpipe Methane (g/kg fuel)	Vehicle A (V3)	3.49	13.35	7.61	5.66	Chassis Only
	Vehicle B (V10)	1.38	12.42	6.04	2.91	Chassis/On-Road
	Vehicle C (V11)	2.10	4.28	3.18	4.13	On-Road Only
	Average	2.32	10.02	5.61	4.23	N.A.
Crankcase Methane (g/kg fuel)	Vehicle A (V3)	22.26	10.84	5.30	3.61	Chassis Only
	Vehicle B (V10)	16.21	7.83	7.31	5.42	Chassis/On-Road
	Vehicle C (V11)	16.90	11.24	6.14	5.70	On-Road Only
	Average	18.46	9.97	6.25	4.91	N.A.
Fuel energy (MJ/mile) *Idle (MJ/hr)	Vehicle A (V3)	164.04*	61.86	46.00	30.15	Chassis Only
	Vehicle B (V10)	193.26*	61.22	35.02	25.20	Chassis/On-Road
	Vehicle C (V11)	215.68*	52.21	32.16	22.91	On-Road Only
	Average	190.99*	58.43	37.73	26.09	N.A.

Table S1-15: Tailpipe and crankcase emissions and dsfc for three 12 L stoichiometric OTR tractors

	Vehicle	Idle	City	Arterial	Highway	Test Methods
Tailpipe Methane (g/kg fuel)	Vehicle A (V23)	0.18	5.07	3.85	3.15	Chassis Only
	Vehicle B (V25)	0.84	2.54	4.16	2.68	Chassis/On-Road
	Vehicle C (V26)	0.63	3.23	1.96	1.16	Chassis/On-Road
	Average	0.55	3.61	3.32	2.33	N.A.
Crankcase Methane (g/kg fuel)	Vehicle A (V23)	15.09	6.72	7.08	6.13	Chassis Only
	Vehicle B (V25)	39.05	8.62	6.20	5.19	Chassis/On-Road
	Vehicle C (V26)	10.42	7.96	6.10	3.72	Chassis/On-Road
	Average	21.52	7.77	6.47	5.01	N.A.
Fuel energy (MJ/mile) *Idle (MJ/hr)	Vehicle A (V23)	200.34*	65.84	42.23	30.03	Chassis Only
	Vehicle B (V25)	81.08*	63.26	40.27	27.61	Chassis/On-Road
	Vehicle C (V26)	320.14*	74.51	44.43	31.85	Chassis/On-Road
	Average	200.52*	67.87	42.31	29.83	N.A.

Table S1-16: Tailpipe and crankcase emissions and dsfc for four 15 L HPDI OTR tractors

	Vehicle	Idle	City	Arterial	Highway	Test Methods
Tailpipe Methane (g/kg fuel)	Vehicle A (V17)	14.77	8.39	6.73	4.44	Chassis/On-Road
	Vehicle B (V18)	10.33	6.29	6.29	4.63	On-Road Only
	Vehicle C (V19)	10.44	5.94	8.16	5.40	On-Road Only
	Vehicle D (V20)	21.03	8.71	4.87	3.53	Chassis/On-Road
	Average	14.14	7.33	6.51	4.50	N.A.
Vent Methane (g/kg fuel)	Average	0.00	22.10	10.15	4.81	N.A.
NG Fuel energy (MJ/mile) *Idle (MJ/hr)	Vehicle A (V17)	136.87*	45.78	26.93	19.47	Chassis/On-Road
	Vehicle B (V18)	184.76*	81.94	19.92	19.98	On-Road Only
	Vehicle C (V19)	253.67*	165.67	19.77	22.68	On-Road Only
	Vehicle D (V20)	170.11*	47.78	34.62	26.22	Chassis/On-Road
	Average	170.11*	85.29	25.31	22.09	N.A.
Total Fuel energy (MJ/mile) *Idle (MJ/hr)	Vehicle A (V17)	221.96*	54.39	29.74	21.52	Chassis/On-Road
	Vehicle B (V18)	304.21*	90.09	22.02	22.16	On-Road Only
	Vehicle C (V19)	418.84*	182.59	21.86	25.17	On-Road Only
	Vehicle D (V20)	177.29*	54.44	37.70	29.10	Chassis/On-Road
	Average	282.39*	94.66	27.86	24.49	N.A.

S1.6. Stasis Scenario to Estimate Emissions

The current inventory and throughput of the CNG and LNG heavy-duty vehicle fleet is not well understood. Our goal was to provide current measurements that could be used to develop emission factors. However, it is important to understand the component level contributions of each source of methane emissions to understand how future reductions can impact emissions. To do this we developed a stasis scenario based on medium fleet growth through 2035. The following sections present the information used to complete the estimation of emissions by component.

S1.6.1 Vehicle Assumptions

1. All transit buses will be powered by CNG ISL G engines or similar engine technologies.
2. All refuse trucks will be powered by CNG ISL G engines or similar engine technologies.
3. The ratio of long haul (regional and interstate) and short haul (local regional) trucks of the OTR trucks was 1:1. This was supported by the latest EPA MOVES vehicle population data for short-haul (963 thousands) and long haul (1,028 thousands) combination trucks.
4. LNG ISL G will power 40% of short-haul trucks and 60% will be powered by CNG ISL G engines.
5. LNG HPDI (2.0), 25% by CNG ISX G, and 25% by LNG ISX G engines will power 50% of long-haul trucks.

Table S1.17 shows the breakdown of vehicles and fuel types for the assumed total population of 908,700. Table S1.18 shows further details for the breakdown of OTR tractors which include both CNG, LNG SI engines and HPDI engines.

Table S1-17: Projected Population of NG Vehicles by Type

Vehicle Type	Refuse (CNG Only)	Transit Bus (CNG Only)	OTR Tractor (CNG/LNG)	Total
Stasis Population	104,000	31,500	773,200	908,700

Table S1-18: Projected Population of NG OTR by Type

Vehicle Category	Short Haul (≤ 320 hp)		Long Haul (> 320 hp)			Total
Population Fraction of HD NG OTR Market	50%		50%			100%
HD NG Engine Technology	SI	SI	SI	HPDI	SI	
Fuel Type	CNG	LNG	CNG	LNG	LNG	
Population Fraction of Vehicle Category	60%	40%	25%	50%	25%	
Population Fraction of Total OTR Tractors	30%	20%	12.5%	25%	12.5%	100%
Stasis Populations	231,960	154,640	96,650	193,300	96,650	773,200

S1.6.2 Station Population Assumptions

The population scenarios for the natural gas stations were developed from multiple sources. These sources included:

- Data reported in literature. For example, the population of CNG and LNG fuel stations for heavy-duty vehicles in 2035 projected by America's Natural Gas Alliance was 12,100 and 700, respectively.
- Based on refueling data of a major natural gas fuel supplier reported by the media: each natural gas station refuels 100 vehicles (may refuel cars and heavy-duty trucks) each day on average.
- Estimates based on literature the statement “the natural gas vehicle market will start to grow aggressively when the percentage of natural gas fuel stations was over 10% of current gasoline fuel stations”. The current population of gasoline stations was about 120,000.
- Estimates based on the assumption of the number of vehicles refueled by each station for different types of transportation services: one fuel station for each 50 refuse trucks (refuse truck fleets were usually small), each 80 transit buses, each 80 short-haul trucks, or each 80 long-haul trucks.

In this scenario, we estimated the population of CNG/LNG stations with the assumption that each CNG (or LNG) fuel station will serve 50 refuse trucks, 80 transit buses, or 80 OTR trucks. The estimated population of NG fuel stations for refuse trucks and transit bus can be found in Table S1-19. The estimated population of CNG and LNG fuel stations for the OTR trucks can be found in Table S1-20. Table S1-21 shows the estimated CNG and LNG fuel stations for HD NG vehicles sector in 2035.

Table S1-19: Projected Population of NG Fuel Stations for HD Natural Gas Refuse Truck and Transit Bus

Vehicle Type		Refuse Truck (CNG only)	Transit Bus (CNG only)
Stasis	Projected population of CNG stations	2080	394

Table S1-20: Projected Population of NG Fuel Stations for HD OTR Trucks

OTR Truck Type		Short Haul		Long Haul		
Vehicle Type		CNG ISL G	LNG ISLG	CNG ISXG	LNG HPDI	LNG ISX G
NG Fuel Station Type		CNG	LNG	CNG	LNG	LNG
Stasis	Projected population of CNG stations	2900	1933	1209	2417	1209

Table S1-21: Projected Population of NG Fuel Stations for HD NG Vehicle Sector

NG Fuel Station Type		CNG	LNG	Total
Stasis	Projected population of CNG stations	6189	5559	11748

S1.6.3 Annual Vehicle Miles Traveled

Table S1-22 shows the AVMT and idle time for each of the vehicle types. Literature data provided estimates for the AVMT. Driving schedules, both chassis dynamometer and in-use data, representative of daily use were processed by the same methods used in this study to find the percentage of idle time. An eight-hour working day was assumed for each vehicle type to determine the average idle time per day.

Table S1-22: AVMT and Idle Time of Each Type of Vehicle

	AVMT (mi)				Idle Time (hr/day)
	City	Arterial	Highway	Total	
Refuse truck	3,775	12,150	9,100	25,000	3.66
Transit bus	2,240	35,320	2,440	40,000	2.29
Short haul OTR truck	725	18,945	30,330	50,000	2.88
Long haul OTR truck	350	6,280	93,370	100,000	1.86

S1.6.4 Station Assumptions

Measured and estimated data from CNG and LNG fueling stations required processing to provide standardized inputs for the estimation model. The estimates presented were based on the following scenarios:

1. Each CNG station refueled 50 refuse trucks, 80 transit buses, or 80 OTR trucks per operational day;
2. Each vehicle refueled once each operational day with six operational days per week for transit buses, and OTR trucks, and five operational days per week for refuse trucks;
3. Annual fuel consumption values were estimated based on the model;

CNG Stations

Methane emissions from CNG fuel stations were estimated for three major emissions sources. The emissions sources included:

1. Methane emissions from dispensing nozzles reported in g/refueling event;
2. Methane emissions from compressors reported in g/kg fuel. The emissions from compressor packing vents, compressor blowdowns, and dryers were categorized into emissions associated with compressor operation;

- Continuous methane leaks (g/day) from sources other than dispensing nozzle and compressors

The estimates presented were based on the following scenarios:

- Each CNG station equipped with two active compressors and one dryer;
- Methane emissions from the dryer and actuator valves, if applicable, were considered as a portion of compressor emissions.

LNG Stations

Methane emissions from LNG fuel stations included those from fuel dispensing nozzles (g/event), manual vehicle tank venting prior to refueling (g/kg fuel), and continuous leaks (g/day). LNG station tank BOG was also a source of emissions, but was a function of more variables and was dependent upon utilization.

S1.6.5 Stasis Emissions Percentage by Component

Table S1-23 presents the summary of emissions (given by percentage of methane lost) for each of the components for both CNG and LNG along with their average combined values.

Table S1-23: Methane Emission for the Stasis Scenario

	Stasis		
	<u>CNG</u>	<u>LNG</u>	<u>Combined</u>
Delivery		<u>0.128%</u>	<u>0.068%</u>
Station Tank BOG		<u>0.100%</u>	<u>0.053%</u>
Station Continuous	<u>0.010%</u>	<u>0.000%</u>	<u>0.005%</u>
Compressor	<u>0.075%</u>		<u>0.035%</u>
Fueling Nozzle	<u>0.003%</u>	<u>0.011%</u>	<u>0.007%</u>
Vehicle Fuel Tank		<u>0.100%</u>	<u>0.053%</u>
Vehicle Manual Vent		<u>0.109%</u>	<u>0.058%</u>
Engine Crankcase	<u>0.698%</u>	<u>0.356%</u>	<u>0.516%</u>
Dynamic Vent		<u>0.226%</u>	<u>0.120%</u>
Engine Tailpipe	<u>0.390%</u>	<u>0.417%</u>	<u>0.404%</u>
Total	<u>1.177%</u>	<u>1.447%</u>	<u>1.321%</u>
CH₄ (MMT)	<u>0.222</u>	<u>0.310</u>	<u>0.532</u>
Fuel (MMT)	<u>18.840</u>	<u>21.452</u>	<u>40.292</u>